inorganics

MDPI

Review

Ferrocene-Based Electrochemical Sensors for Cations

Angel A. J. Torriero * and Ashwin K. V. Mruthunjaya

School of Life and Environmental Sciences, Deakin University, Burwood, VIC 3125, Australia
* Correspondence: angel.torriero@deakin.edu.au; Tel.: +61-3-9244-6897

Abstract: This study investigates novel ferrocene-based electrochemical sensors for metal cation detection via the design, synthesis and characterisation of ferrocene derivatives. Specifically, this research determines the redox potentials of ferrocene versus decamethylferrocene to provide insight into the redox potential variations. The investigation also examines how electrochemical oxidation of the ferrocene moiety can modulate host affinity for transition metal cations via effects such as electrostatic interactions and changes to coordination chemistry. Metal ion coordination to receptors containing functional groups like imine and quinoline is explored to elucidate selectivity mechanisms. These findings advance the fundamental understanding of ferrocene electrochemistry and host–guest interactions, supporting the development of improved cation sensors with optimised recognition properties, sensitivity and selectivity. Overall, this work lays the necessary groundwork for applications in analytical chemistry and sensor technologies via customised ferrocene-derived materials.

Keywords: ferrocene; electrochemical sensors; metal cation; host–guest interaction

check for updates

Citation: Torriero, A.A.J.; Mruthunjaya, A.K.V. Ferrocene - Based Electrochemical Sensors for Cations. *Inorganics* **2023**, *11*, 472. https://doi.org/10.3390/inorganics11120472

Academic Editors: Mojca Čakić Semenčić and Lidija Barišić

Received: 11 November 2023
Revised: 29 November 2023
Accepted: 30 November 2023
Published: 4 December 2023

1. Introduction

The landscape of molecular sensing and recognition has been redefined by the versatile synthetic chemistry of ferrocene (Fc), an organometallic compound that has emerged as a cornerstone in developing electrochemical molecular receptors for various cationic species [1–5]. The fascination with Fc in this context stems from its well-established synthetic routes and the accessibility of its redox couple, which confers it with exceptional utility for constructing molecular receptors. These receptors often incorporate Fc functionalities strategically, serving as signalling or reporter groups. The redox responses of these functionalities undergo perturbations upon binding guest molecules. Alternatively, Fc can serve as a structural component, allowing for precise control over the topology of the guest binding site. Remarkably, Fc-based receptors, especially those assuming dual roles, exhibit diverse functionalities that transcend the capabilities of purely organic architectures [6].

The design paradigm for redox-active receptors commonly employs spacer groups that covalently link the host (metal ion binding moieties) to the Fc unit. This strategic arrangement capitalises on the coexistence of the redox-active centre and the receptor functionality within the same molecular entity. This framework enables Fc-based molecular receptors to engage in concurrent or sequential processes of electron transfer and guest binding (guest = metal cations), with their mutual influence particularly evident between alkali and alkaline earth metal ions and crown ether or similar oxygen-containing ligands. However, recent investigations have revealed that when hosts containing amine functionalities are involved (e.g., cyclen and cyclam), the interplay between electron transfer and molecular recognition takes on a more intricate nature [7–10].

Fc-based molecular receptors can be designed to bind anionic, cationic or neutral guest molecules [11,12]. Nevertheless, this review article explores Fc-based sensors and molecular receptors tailored for cationic species, shedding light on their intricate designs, redox mechanisms and sensing responses. We examine the foundational reasons underlying the suitability of Fc as a molecular scaffold for this task, considering factors such as the effect of solvents and substituents on Fc redox potential. We discuss the interactions between Fc

and crown ethers as opposed to amine-containing hosts and illustrate these concepts using concrete sensor examples, outlining the resultant changes in electrochemical potentials. By navigating through relevant literature and dissecting prominent case studies, we aim to provide an overview of the advancements in electrochemical Fc-based sensing platforms. Via this exploration, we unveil the intricate mechanisms governing their operation and emphasise their pivotal role in shaping the modern landscape of molecular sciences.

2. Why Ferrocene?

Ferrocene stands out because of its unique structure: a central iron atom neatly sandwiched between two cyclopentadienyl rings. This structural arrangement leads to some fascinating electrochemical properties that have attracted the curiosity of many researchers. The redox potential of Fc, as discussed below, is known to vary based on its proximity to the host. This observation, although noteworthy, is not an isolated phenomenon. When diving deeper into the electrochemical behaviour of Fc, it becomes apparent that several other factors also affect the mentioned redox potential. These factors include the nature of the solvent, the type of supporting electrolyte employed, and the specific substituents connected to the Fc molecule. The strong ability of Fc to exhibit changes in its electrochemical responses under these varied conditions highlights its versatility and has strengthened its place as a subject of intense study in electrochemistry.

In the extensive body of research surrounding Fc, one aspect has been given less prominence than it deserves: the role of the solvent in modulating Fc redox potential. While ferrocene is often put on a pedestal as an internal reference redox scale or system (IRRS), it is crucial to take a step back and consider the entirety of the system, including the solvent. Neglecting or underestimating the influence of the solvent could lead to a biased or incomplete picture of how ferrocene behaves in different experimental setups. These interactions involve intricate electrostatic interplays between the solvent or electrolyte and specific components of the ferrocene molecule. Such interactions encompass the iron centre and the cyclopentadienyl ring components [13]. Research by Yang et al. shed light on this phenomenon via a comprehensive analysis of the molecular electrostatic potential (MEP) of Fc and its oxidised ferrocenium ion (Fc^+ or $[Fe^{III}(\eta^5\text{-}C_5H_5)_2]^+$) counterpart [14]. The study elucidated the distribution of electrostatic charges, revealing remarkable insights into the solvation behaviour of Fc. The MEP analysis uncovered negative electrostatic potentials concentrated atop the cyclopentadienyl rings alongside a distinctive planetary-like charge distribution encircling the central iron atom. This distribution significantly fosters electrostatic interactions between Fc and positively charged molecules or ions, including those with electron-acceptor functionalities. Notably, the positively charged regions on the sides of the cyclopentadienyl rings facilitate interactions with electron-donating components from the surrounding solvent or electrolyte.

Interestingly, in the case of Fc^+, the MEP analysis distinctly presents positive electrostatic potentials. This configuration favours electrostatic interactions between Fc^+ and negatively charged ions or molecules characterised by electron-donor groups. The discernible MEP differences between Fc and its Fc^+ counterpart assume a pivotal role, elucidating the observed variances in mass transport properties within viscous solvents, such as ionic liquids [15–19]. This intricate understanding of solvation effects and their consequential impact on Fc and Fc^+ behaviour in distinct environments holds significant promise for advancing our comprehension of their behaviour in diverse contexts. One of which is the demystification of Fc as the optimal IRRS. An IRRS is a reversible or nearly reversible redox system that provides a known and stable, solvent-independent reference point in non-aqueous solvents where reliable reference electrodes are difficult to establish or stabilise [19–21]. The IRRS is generally used in conjunction with a quasi-reference electrode [22–27].

The history of establishing an IRRS that remains unaffected by the solvent for comparing redox potentials in non-aqueous systems is extensive. This chronicle commenced with the introduction of the $Rb|Rb^+$ or $Rb(Hg)|Rb^+$ redox couples and subsequently

advanced with the proposition of employing organometallic redox pairs [28]. To streamline the comparative process and enhance simplicity, IUPAC advocated for the adoption of specific IRRS in non-aqueous contexts, namely Fc/Fc^+ (also referred to as $Fc^{0/+}$) and bis(biphenyl)chromium(0) | bis(biphenyl)chromium(I) [28]. This selection was made arbitrarily from various published redox systems [28]. It is noteworthy to observe how an initial arbitrary selection of redox systems, including Fc, has permeated the present scientific landscape, leading to the enduring perception of Fc as an incontrovertible IRRS. This underscores the intricate interplay between historical conventions, pragmatic considerations and the trajectory of scientific understanding that collectively shape the enduring reputation of Fc.

A range of essential attributes characterises an effective IRRS, several initially outlined by Gritzner and Kuta in the IUPAC recommendation [28]. Additionally, a revised set of properties has been introduced by our research group [29]. This updated framework expands and refines the criteria that define a reliable IRRS, reflecting advancements in our understanding and methodological approaches. The evolution of these properties demonstrates the maturation of the field and underscores the commitment to enhancing the accuracy and applicability of IRRS in diverse electrochemical settings.

Decamethylferrocene (DmFc or $[Fe^{II}(\eta^5\text{-}C_5(CH_3)_5)_2]$) exhibits notably diminished solvent–solute interactions in organic solvent systems, a contrast that surpasses at least one order of magnitude in comparison to ferrocene. This divergence arises due to the methyl-substituent groups within the cyclopentadienyl rings of DmFc, which effectively impede both specific and non-specific interactions. This obstruction originates from the hindered accessibility of organic solvent and supporting electrolyte molecules to the metal centre and the cyclopentadienyl ring [13,30–32]. The veracity of this observation is further corroborated by the analysis of X-ray diffraction patterns of DmFc, which substantiates that the inter-ring methyl groups within DmFc adhere to Van der Waals distances [33]. Consequently, owing to its intrinsic characteristics, DmFc proves to be more appropriate than Fc as an IRRS within organic solvents, where it undergoes a reversible one-electron oxidative transfer process, leading to the formation of decamethylferrocenium ($DmFc^+$ or $[Fe^{III}(\eta^5\text{-}C_5(CH_3)_5)_2]^+$), which is reduced back to DmFc when the potential scanning direction is reverted. The $DmFc^{0/+}$ mid-point potential value (E_m) associated with this electron transfer is lower than that of Fc due to the electron-donating influence imparted by the methyl groups (inductive effect). These methyl groups direct electron density towards the metal ion, facilitating the extraction of an electron by the electrode. Table 1 shows the difference in the E_m values between $Fc^{0/+}$ and $DmFc^{0/+}$, which fluctuates from 0.614 ± 0.005 V in dichloromethane/0.1 M $[Bu_4N][TFAB]$ ($[TFAB] = [B(C_6F_5)_4]^-$) to 0.413 ± 0.005 V in tetrahydrofuran/0.1 M $[Bu_4N][BF_4]$, representing a difference of 0.201 V due to solvent and supporting electrolyte effects. Furthermore, a change of 0.152 V can be observed by transitioning from tetrahydrofuran to 2,2,2-trifluoroethanol as the organic solvent while maintaining constant the nature and concentration (0.1 M $[Bu_4N][ClO_4]$) of the supporting electrolyte. To mitigate uncertainties when comparing E_m in Table 1, all potential values cited are referenced against the $DmFc^{0/+}$ potential scale. Consequently, as the values in this table signify the disparity in E_m, the chances exist for the absolute E_m values of the $Fc^{0/+}$ and $DmFc^{0/+}$ IRRS to exhibit a more significant variation than that presented here.

When considering the impact of substituents on the cyclopentadienyl rings, the solvent role becomes even more pronounced. Substituents modulate the electron density around the iron centre via their electron-donating or -withdrawing nature. This change in electron density, in turn, can influence the solvation shell and the nature of solvent interactions with ferrocene and its derivatives (Table 2). For instance, an electron-donating substituent might increase the negative charge density on the cyclopentadienyl ring. In a polar solvent, which already affects the redox potential of Fc via the stabilisation of charged species, the increase in negative charge might result in an even more pronounced shift of its E_m to more negative potential values. However, the effect might be attenuated or manifest differently

in a non-polar solvent. Conversely, electron-withdrawing substituents could exacerbate or mitigate solvent effects, contingent on the specific properties of the solvent used and the nature of the substituent. The interplay between solvent effects and substituent-induced electronic modulation offers a dynamic continuum, with each factor potentially amplifying or modulating the other, resulting in a rich variability of electrochemical behaviour.

Table 1. Redox potentials of Fc vs. $DmFc^{0/+}$ IRRS in different organic solvents containing different supporting electrolytes.

Solvent	Electrolyte	E_m of $Fc^{0/+}$ vs. $DmFc^{0/+}$(V)	Ref.
1,2-dibromoethane	0.1 M $[Bu_4N][ClO_4]$	0.475 ± 0.007	[13]
1,2-dichloroethane	0.1 M $[Bu_4N][ClO_4]$	0.532 ± 0.001	[13]
1,2-dichlorobenzene	0.1 M $[Bu_4N][ClO_4]$	0.535 ± 0.001	[13]
2-propanol	0.1 M $[Bu_4N][CF_3SO_3]$	0.455 ± 0.003	[13]
2,2,2-trifluoroethanol	0.1 M $[Bu_4N][ClO_4]$	0.575 ± 0.004	[13]
Acetone	0.1 M $[Bu_4N]Cl$	0.451 ± 0.005	[34]
	0.1 M $[Bu_4N][ClO_4]$	0.479 ± 0.004	[13]
	0.1 M $[Bu_4N][PF_6]$	0.487 ± 0.005	[34]
	0.1 M $[Bu_4N]$[TFAB]	0.504 ± 0.005	[34]
Acetonitrile (CH_3CN)	0.1 M $[Bu_4N]Cl$	0.501 ± 0.005	[34]
	0.1 M $[Bu_4N][ClO_4]$	0.505 ± 0.002	[13]
	0.1 M $[Bu_4N][PF_6]$	0.509 ± 0.003	[35]
	0.1 M $[Bu_4N]$[TFAB]	0.517 ± 0.005	[34]
Acetonitrile/dichloromethane (80:20)	0.1 M $[Bu_4N][PF_6]$	0.512 ± 0.003	[36]
Aniline	0.1 M $[Bu_4N][ClO_4]$	0.527 ± 0.004	[13]
Anisole	0.1 M $[Bu_4N][PF_6]$	0.518 ± 0.005	[34]
	0.1 M $[Bu_4N]$[TFAB]	0.607 ± 0.005	[34]
Benzonitrile	0.1 M $[Bu_4N]Cl$	0.524 ± 0.005	[34]
	0.1 M $[Bu_4N][ClO_4]$	0.523 ± 0.001	[13]
	0.1 M $[Bu_4N][PF_6]$	0.530 ± 0.005	[34]
	0.1 M $[Bu_4N]$[TFAB]	0.543 ± 0.005	[34]
Benzyl alcohol	0.1 M $[Bu_4N][ClO_4]$	0.508 ± 0.003	[13]
Bromobenzene	0.1 M $[Bu_4N][ClO_4]$	0.489 ± 0.005	[13]
Chlorobenzene	0.1 M $[Bu_4N][ClO_4]$	0.497 ± 0.001	[13]
Chloroform	0.1 M $[Bu_4N][ClO_4]$	0.483 ± 0.001	[13]
Dichloromethane (DCM)	0.1 M $[Bu_4N]Cl$	0.534 ± 0.005	[34]
	0.1 M $[Bu_4N][ClO_4]$	0.532 ± 0.002	[13]
	0.1 M $[Bu_4N][ClO_4]$	0.570 ± 0.002	[2]
	0.1 M $[Bu_4N][PF_6]$	0.548 ± 0.003	[35]
	0.1 M $[Et_4N][BF_4]$	0.541 ± 0.003	[17]
	0.1 M $[Bu_4N]$[TFAB]	0.614 ± 0.005	[34]
	0.1 M $[C_4mPyr]$[FAP]	0.589 ± 0.003	[17]
	0.1 M $[C_2mim]$[FAP]	0.590 ± 0.003	[17]
	0.1 M $[C_2mim][B(CN)_4]$	0.588 ± 0.003	[17]
	0.1 M $[C_4mim][NTf_2]$	0.570 ± 0.003	[17]
	0.1 M $[C_4mPyr][NTf_2]$	0.568 ± 0.003	[17]
	0.1 M $[C_2mim]$[FSI]	0.569 ± 0.003	[17]
	0.1 M $[C_3mim]$[FSI]	0.568 ± 0.003	[17]
	0.1 M $[C_4mPyr][N(CN)_2]$	0.564 ± 0.003	[17]
	0.1 M $[C_4mim][PF_6]$	0.556 ± 0.003	[17]
	0.1 M $[C_4mim][BF_4]$	0.557 ± 0.003	[17]
	0.1 M $[C_4mim][CF_3SO_3]$	0.556 ± 0.003	[17]

Table 1. *Cont.*

Solvent	Electrolyte	E_m of $Fc^{0/+}$ vs. $DmFc^{0/+}$ (V)	Ref.
Diethyl ether	0.1 M $[Bu_4N][BArF_{24}]$	0.550 ± 0.005	[34]
	0.1 M $Na[BArF_{24}]$	0.583 ± 0.005	[34]
Dimethyl sulfoxide	0.1 M $[Bu_4N][PF_6]$	0.486 ± 0.005	[34]
	0.1 M $[Bu_4N]$[TFAB]	0.493 ± 0.005	[34]
	0.1 M $[Bu_4N][ClO_4]$	0.468 ± 0.001	[13]
Ethanol	0.1 M $[Bu_4N][ClO_4]$	0.473 ± 0.005	[13]
Formamide	0.1 M $[Bu_4N][ClO_4]$	0.510 ± 0.003	[13]
Methanol (MeOH)	0.1 M $[Bu_4N][ClO_4]$	0.497 ± 0.002	[13]
Nitrobenzene	0.1 M $[Bu_4N][ClO_4]$	0.514 ± 0.002	[13]
Nitromethane	0.1 M $[Bu_4N]Cl$	0.505 ± 0.005	[34]
	0.1 M $[Bu_4N][ClO_4]$	0.516 ± 0.004	[13]
	0.1 M $[Bu_4N][PF_6]$	0.510 ± 0.005	[34]
	0.1 M $[Bu_4N]$[TFAB]	0.516 ± 0.005	[34]
N-methylformamide	0.1 M $[Bu_4N][ClO_4]$	0.510 ± 0.002	[13]
N,N-dimethylformamide (DMF)	0.1 M $[Bu_4N]Cl$	0.475 ± 0.005	[34]
	0.1 M $[Bu_4N][ClO_4]$	0.458 ± 0.003	[13]
	0.1 M $[Bu_4N][PF_6]$	0.478 ± 0.005	[34]
	0.1 M $[Bu_4N]$[TFAB]	0.493 ± 0.005	[34]
N,N-dimethylacetamide	0.1 M $[Bu_4N][ClO_4]$	0.455 ± 0.008	[13]
Propylene carbonate	0.1 M $[Bu_4N][ClO_4]$	0.495 ± 0.002	[13]
Pyridine	0.1 M $[Bu_4N][ClO_4]$	0.517 ± 0.004	[13]
Tetrahydrofuran	0.1 M $[Bu_4N][BF_4]$	0.413 ± 0.005	[34]
	0.1 M $[Bu_4N][CF_3SO_3]$	0.438 ± 0.005	[34]
	0.1 M $[Bu_4N][ClO_4]$	0.423 ± 0.005	[34]
		0.427 ± 0.002	[13]
	0.1 M $[Bu_4N][PF_6]$	0.446 ± 0.005	[34]
	0.1 M $[Bu_4N][BPh_4]$	0.485 ± 0.005	[34]
	0.1 M $Na[BArF_{24}]$	0.502 ± 0.005	[34]
	0.1 M $[Bu_4N]$[TFAB]	0.484 ± 0.005	[34]
	0.1 M $[Bu_4N][BArF_{24}]$	0.521 ± 0.005	[34]
Toluene	0.1 M $[Bu_4N][BF_4]$ [a]	0.430 ± 0.005	[34]

Abbreviations: $[Bu_4N]$ = tetrabutylammonium; $[PF_6]$ = hexafluorophosphate; $[ClO_4]$ = perchlorate; $[BF_4]$ = tetrafluoroborate; $[CF_3SO_3]$ = trifluoromethanesulfonate; [TFAB] = tetrakis(pentafluorophenyl)borate; $[Et_4N]$ = tetraethylammonium; $[C_4mPyr]$ = 1-butyl-1-methylpyrrolidinium; $[C_2mim]$ = -ethyl-3-methylimidazolium; $[C_4mim]$ = 1-butyl-3-methylimidazolium; [FAP] = tris(pentafluoroethyl)trifluorophosphate; $[B(CN)_4]$ = tetracyanoborate; $[NTf_2]$ = bis(trifluoromethanesulfonyl)amide; [FSI] = bis(fluorosulfonyl)imide; $[N(CN)_2]$ = dicyanamide; $[BArF_{24}]$ = tetrakis(3,5-bis(trifluoromethyl)phenyl)borate; $[BPh_4]$ = tetraphenylborate. [a] the toluene:$[Bu_4N][BF_4]$ electrolyte is of the 3:1 stoichiometry.

The influence of substituents on the E_m of Fc is an exciting aspect of molecular electrochemistry that warrants in-depth investigation. It is well-established that the electron density around the central iron atom can be modulated by introducing various substituents on the surrounding ligands. Depending on the electronic nature of the substituent, such modulation can either stabilise or destabilise the oxidised form of the complex, and its effects rest predominantly upon the electronic principles of induction. When an electron-donating group is appended to the cyclopentadienyl ring of Fc, it can engage in inductive donation. This introduces electron density to the π-system of the cyclopentadienyl ring, which in turn delocalises to the central iron atom. Such an electron density enhancement around the metal cation predisposes it to a greater likelihood of electron loss, making oxidation more favourable, thus shifting the E_m to more negative potential values than unmodified Fc (Table 2).

In contrast, electron-withdrawing groups operate on induction and resonance withdrawal principles. These groups extract electron density from the cyclopentadienyl ring. Additionally, certain withdrawing groups can engage in resonance structures that pull electron density away from the cyclopentadienyl ring and into the substituent. As a result of this electron density diminishment, the central iron cation becomes less prone to losing an electron, translating to a shift of the E_m to more positive potential values with respect to that of unmodified Fc (Table 2).

Table 2 shows the E_m values of different substituted Fc derivatives versus $Fc^{0/+}$, which is equal to −0.570 V vs. $Fc^{0/+}$ IRRS for DmFc in dichloromethane/0.1 M $[Bu_4N][ClO_4]$ and 0.640 V vs. $Fc^{0/+}$ for 1,1′-bis(trifluoromethyl)ferrocene in the same solvent/supporting electrolyte system, representing a difference of 1.21 V. Furthermore, a change of 0.141 V can be observed for 1,1′,3,3′-tetra(*t*-butyl)ferrocene by transitioning from acetonitrile (0.1 M $[Bu_4N][ClO_4]$) to toluene containing 0.5 M $[Hex_4N][ClO_4]$ as the supporting electrolyte.

The E_m of Fc is also affected by the distance between the ferrocenyl moiety and substituents that either donate or withdraw electrons [10,37,38]. When analysing a scenario where an electron-withdrawing group is attached to the Fc unit (e.g., Fc-COOH), it becomes evident that increasing the number of methylene groups progressively diminishes the electron-withdrawing effect on Fc—specifically, introducing a single methylene group between the Fc and the carboxylic group results in an E_m shift of 0.245 V towards more negative potential values (Table 2). The magnitude of this shift reduces upon subsequent additions of methylene groups, with further negative shifts of 0.016 and 0.025 V observed following the incorporation of a second and third methylene unit, respectively. In this new scenario (e.g., Fc-$(CH_2)_3$-COOH), the inductive donating property of methylene towards the cyclopentadienyl rings of Fc begins to dominate the resultant E_m of Fc.

The resultant molecule often exhibits compromised stability when the Fc unit is directly linked with electron-donating groups such as amines or hydroxyls. This is exemplified by Fc-NH_2, whose stability depends on various factors such as temperature, pH, and the presence of oxidising agents (e.g., oxygen from the air). Consequently, research on these molecule families typically commences with one methylene unit, as seen in Fc-CH_2-OH and Fc-CH_2-NH_2 (Table 2). Interestingly, the observed E_m shift magnitude towards negative values closely aligns with those exhibited by Fc connected to carboxylic groups bearing variable counts of methylene groups as a bridge. As an illustration, the negative E_m shifts of 0.041, 0.032 and 0.040 V are documented upon increasing the number of methylene groups from Fc-CH_2-COOH, Fc-CH_2-NH_2 and Fc-CH_2-OH to Fc-$(CH_2)_3$-COOH, Fc-$(CH_2)_3$-NH_2 and Fc-$(CH_2)_3$-OH, respectively.

From these observations, it is possible to deduct the pivotal role of methylene group quantity in shaping the overall reactivity and behaviour of ferrocene-based compounds. Expanding the methylene chain effectively serves as a strategic buffer, isolating the electron-withdrawing effects and safeguarding the inherent chemical stability of Fc. Conversely, the judicious placement of electron-donating entities proximal to the ferrocene unit presents opportunities to modulate its E_m and alter its oxidation pathway (see below).

Furthermore, it is essential to consider the spatial orientation and steric hindrance offered by substituents. While electronic effects often dominate, steric factors can influence the approach and interaction of molecules at the electrode surface during redox processes, potentially altering observed redox potentials. Thus, while the electronic properties of substituents provide a foundational understanding of their effects on redox potential, the holistic picture must also account for three-dimensional spatial factors.

Table 2. Redox potentials of substituted Fc in different organic solvents containing different supporting electrolytes.

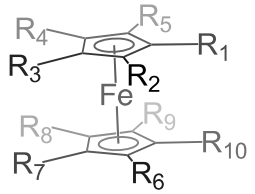	**Solvent**	**Electrolyte**	E_m **vs. Fc$^{0/+}$ (V)**	**Ref**
$\mathbf{R}_{1–10}$: H	DCM	0.1 M $[Bu_4N][ClO_4]$	0.000	[2]
$\mathbf{R}_{1–10}$: CH_3	DCM	0.1 M $[Bu_4N][ClO_4]$	−0.570	[2]
$\mathbf{R}_{1–5}$: CH_3; $\mathbf{R}_{6–10}$: H	DCM	0.1 M $[Bu_4N][ClO_4]$	−0.270	[2]
$\mathbf{R}_{1,10}$: CH_3; $\mathbf{R}_{2–9}$: H	CH_3CN	0.1 M $[Bu_4N][ClO_4]$	−0.113	[39]
	CH_3CN	0.1 M $[Bu_4N][PF_6]$	−0.096	[40]
	MeOH	0.1 M $[Bu_4N][ClO_4]$	−0.104	[39]
	Toluene	0.5 M $[Hex_4N][ClO_4]$	−0.075	[39]
$\mathbf{R}_{2–9}$: CH_3; $\mathbf{R}_{1,10}$: H	CH_3CN	0.1 M $[Bu_4N][PF_6]$	−0.406	[40]
$\mathbf{R}_{1,3,7,10}$: *t*-Bu; $\mathbf{R}_{2,4,5,6,8,9}$: H	CH_3CN	0.1 M $[Bu_4N][ClO_4]$	−0.238	[39]
	CH_3CN	0.1 M $[Bu_4N][PF_6]$	−0.233	[40]
	MeOH	0.1 M $[Bu_4N][ClO_4]$	−0.229	[39]
	Toluene	0.5 M $[Hex_4N][ClO_4]$	−0.097	[39]
$\mathbf{R}_1$: *n*-Bu; $\mathbf{R}_{2–10}$: H	CH_3CN	0.1 M $[Bu_4N][ClO_4]$	−0.062	[39]
	MeOH	0.1 M $[Bu_4N][ClO_4]$	−0.055	[39]
	Toluene	0.5 M $[Hex_4N][ClO_4]$	−0.073	[39]
$\mathbf{R}_{1–10}$: CH_2Ph	DCM	0.1 M $[Bu_4N][ClO_4]$	−0.070	[2]
$\mathbf{R}_{1,10}$: CF_3; $\mathbf{R}_{2–9}$: H	DCM	0.1 M $[Bu_4N][ClO_4]$	0.640	[2]
$\mathbf{R}_1$: $CH{=}CH_2$; $\mathbf{R}_{2–10}$: H	CH_3CN	0.1 M $[Et_4N][ClO_4]$	0.022	[41]
$\mathbf{R}_1$: CH_2OH; $\mathbf{R}_{2–10}$: H	CH_3CN	0.1 M $[Et_4N][ClO_4]$	0.029	[41]
	CH_3CN	0.1 M $[Bu_4N][ClO_4]$	−0.012	[39]
	CH_3CN	0.1 M $[Bu_4N][PF_6]$	0.016	[38]
	MeOH	0.1 M $[Bu_4N][ClO_4]$	0.005	[39]
	Toluene	0.5 M $[Hex_4N][ClO_4]$	−0.044	[39]
$\mathbf{R}_1$: $(CH_2)_2OH$; $\mathbf{R}_{2–10}$: H	CH_3CN	0.1 M $[Bu_4N][PF_6]$	−0.046	[38]
$\mathbf{R}_1$: $(CH_2)_3OH$; $\mathbf{R}_{2–10}$: H	CH_3CN	0.1 M $[Bu_4N][PF_6]$	−0.052	[38]
$\mathbf{R}_1$: $(CH_2)_4OH$; $\mathbf{R}_{2–10}$: H	CH_3CN	0.1 M $[Bu_4N][PF_6]$	−0.054	[38]
$\mathbf{R}_1$: $CH(CH_3)OH$; $\mathbf{R}_{2–10}$: H	CH_3CN	0.1 M $[Et_4N][ClO_4]$	−0.008	[41]
$\mathbf{R}_{1,10}$: $CH(CH_3)OH$; $\mathbf{R}_{2–9}$: H	CH_3CN	0.1 M $[Et_4N][ClO_4]$	−0.013	[41]
$\mathbf{R}_1$: CH_2CONH_2; $\mathbf{R}_{2–10}$: H	CH_3CN	0.1 M $[Bu_4N][PF_6]$	−0.003	[38]
$\mathbf{R}_1$: $(CH_2)_2CONH_2$; $\mathbf{R}_{2–10}$: H	CH_3CN	0.1 M $[Bu_4N][PF_6]$	−0.027	[38]
$\mathbf{R}_1$: $(CH_2)_3CONH_2$; $\mathbf{R}_{2–10}$: H	CH_3CN	0.1 M $[Bu_4N][PF_6]$	−0.049	[38]
$\mathbf{R}_1$: COOH; $\mathbf{R}_{2–10}$: H	CH_3CN	0.1 M $[Et_4N][ClO_4]$	0.239	[41]
	CH_3CN	0.1 M $[Bu_4N][ClO_4]$	0.234	[39]
	CH_3CN	0.1 M $[Li][ClO_4]$	0.239	[37]
	MeOH	0.1 M $[Bu_4N][ClO_4]$	0.233	[39]
	Toluene	0.5 M $[Hex_4N][ClO_4]$	0.157	[39]
$\mathbf{R}_1$: CH_2COOH; $\mathbf{R}_{2–10}$: H	CH_3CN	0.1 M $[Li][ClO_4]$	−0.006	[37]
$\mathbf{R}_1$: $(CH_2)_2COOH$; $\mathbf{R}_{2–10}$: H	CH_3CN	0.1 M $[Li][ClO_4]$	−0.022	[37]
$\mathbf{R}_1$: $(CH_2)_3COOH$; $\mathbf{R}_{2–10}$: H	CH_3CN	0.1 M $[Li][ClO_4]$	−0.047	[37]

Table 2. *Cont.*

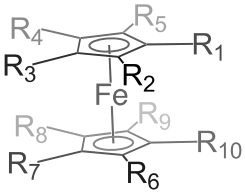	**Solvent**	**Electrolyte**	E_m **vs. Fc$^{0/+}$ (V)**	**Ref**
R$_1$: $COOCH_3$; **R**$_{2–10}$: H	CH_3CN	0.1 M $[Et_4N][ClO_4]$	0.243	[41]
	CH_3CN	0.1 M $[Bu_4N][ClO_4]$	0.237	[39]
	MeOH	0.1 M $[Bu_4N][ClO_4]$	0.263	[39]
	Toluene	0.5 M $[Hex_4N][ClO_4]$	0.214	[39]
R$_{1,10}$: $COOCH_3$; **R**$_{2–9}$: H	CH_3CN	0.1 M $[Et_4N][ClO_4]$	0.470	[41]
R$_1$: $COCH_3$; **R**$_{2–10}$: H	CH_3CN	0.1 M $[Bu_4N][ClO_4]$	0.244	[39]
	MeOH	0.1 M $[Bu_4N][ClO_4]$	0.271	[39]
	Toluene	0.5 M $[Hex_4N][ClO_4]$	0.191	[39]
R$_{1,10}$: $COCH_3$; **R**$_{2–9}$: H	CH_3CN	0.1 M $[Et_4N][ClO_4]$	0.482	[41]
R$_1$: COPh; **R**$_{2–10}$: H	CH_3CN	0.1 M $[Bu_4N][ClO_4]$	0.250	[39]
	MeOH	0.1 M $[Bu_4N][ClO_4]$	0.272	[39]
	Toluene	0.5 M $[Hex_4N][ClO_4]$	0.214	[39]
R$_1$: $CONH_2$; **R**$_{2–10}$: H	CH_3CN	0.1 M $[Bu_4N][PF_6]$	0.183	[38]
R$_1$: CHO; **R**$_{2–10}$: H	CH_3CN	0.1 M $[Bu_4N][ClO_4]$	0.285	[39]
	MeOH	0.1 M $[Bu_4N][ClO_4]$	0.304	[39]
	Toluene	0.5 M $[Hex_4N][ClO_4]$	0.259	[39]
R$_1$: CH_2NH_2; **R**$_{2–10}$: H	CH_3CN	0.1 M $[Bu_4N][PF_6]$	−0.014	[38]
R$_1$: $(CH_2)_2NH_2$; **R**$_{2–10}$: H	CH_3CN	0.1 M $[Bu_4N][PF_6]$	−0.037	[38]
R$_1$: $(CH_2)_3NH_2$; **R**$_{2–10}$: H	CH_3CN	0.1 M $[Bu_4N][PF_6]$	−0.046	[38]
R$_1$: $(CH_2)_4NH_2$; **R**$_{2–10}$: H	CH_3CN	0.1 M $[Bu_4N][PF_6]$	−0.060	[38]
R$_1$: $CH_2N(CH_3)_2$; **R**$_{2–10}$: H	CH_3CN	0.1 M $[Bu_4N][ClO_4]$	−0.004	[39]
	MeOH	0.1 M $[Bu_4N][ClO_4]$	0.046	[39]
	Toluene	0.5 M $[Hex_4N][ClO_4]$	0.009	[39]
	CH_3CN	0.1 M $[Bu_4N][PF_6]$	−0.023	[42]
	DCM:CH_3CN 1:4	0.1 M $[Bu_4N][PF_6]$	0.003	[7]
R$_{1,10}$: $CH_2N(CH_3)_2$; **R**$_{2–9}$: H	CH_3CN	0.1 M $[Bu_4N][PF_6]$	−0.017	[42]
R$_{1,10}$: $(CH_2)_2N(CH_3)_2$; **R**$_{2–9}$: H	CH_3CN	0.1 M $[Bu_4N][PF_6]$	−0.077	[42]
R$_{1,10}$: $CH_2N(CH_2Ph)_2$; **R**$_{2–9}$: H	DCM	0.2 M $[Bu_4N][PF_6]$	−0.001	[9]
R$_{1,10}$: $C(CH_3)=N(CH_2)_5CH_3$; **R**$_{2–9}$: H	DCM:CH_3CN 1:1	0.1 M $[Bu_4N][PF_6]$	0.211	[43]
R$_{1,10}$: 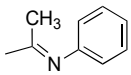 ; **R**$_{2–9}$: H	DCM:CH_3CN 1:1	0.1 M $[Bu_4N][PF_6]$	0.289	[43]
R$_{1,10}$: 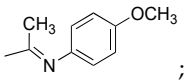 ; **R**$_{2–9}$: H	DCM:CH_3CN 1:1	0.1 M $[Bu_4N][PF_6]$	0.245	[43]
R$_{1,10}$: 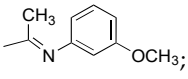 ; **R**$_{2–9}$: H	DCM:CH_3CN 1:1	0.1 M $[Bu_4N][PF_6]$	0.261	[43]
R$_{1,10}$: 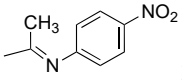 ; **R**$_{2–9}$: H	DCM:CH_3CN 1:1	0.1 M $[Bu_4N][PF_6]$	0.435	[43]
R$_{1,10}$: 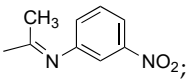 ; **R**$_{2–9}$: H	DCM:CH_3CN 1:1	0.1 M $[Bu_4N][PF_6]$	0.390	[43]
R$_{1,10}$: SH; **R**$_{2–9}$: H	DCM	0.1 M $[Bu_4N][ClO_4]$	0.200	[2]

Table 2. *Cont.*

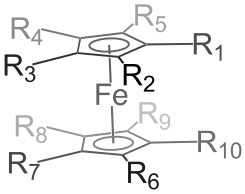	**Solvent**	**Electrolyte**	E_m **vs. Fc$^{0/+}$ (V)**	**Ref**
R$_1$: $S(CH_2)_2OH$; **R**$_{2–10}$: H	CH_3CN	0.1 M $[Et_4N][ClO_4]$	0.010	[41]
R$_1$: $SCH_2CH(CH_3)COOH$; **R**$_{2–10}$: H	CH_3CN	0.1 M $[Et_4N][ClO_4]$	0.039	[41]
R$_1$: $CH(CH_3)SPh$; **R**$_{2–10}$: H	CH_3CN	0.1 M $[Et_4N][ClO_4]$	0.020	[41]
R$_1$: CH(Ph)SPh; **R**$_{2–10}$: H	CH_3CN	0.1 M $[Et_4N][ClO_4]$	0.043	[41]
R$_1$: 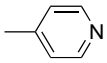 ; **R**$_{2–10}$: H	CH_3CN	0.1 M $[Bu_4N][ClO_4]$	0.180	[44]
R$_{1,10}$: 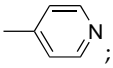 ; **R**$_{2–9}$: H	CH_3CN	0.1 M $[Bu_4N][ClO_4]$	0.350	[44]
R$_1$: 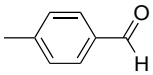 ; **R**$_{2–10}$: H	CH_3CN	0.1 M $[Bu_4N][ClO_4]$	0.170	[44]
R$_{1,10}$: 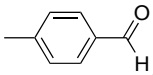 ; **R**$_{2–9}$: H	CH_3CN	0.1 M $[Bu_4N][ClO_4]$	0.180	[44]
R$_1$: 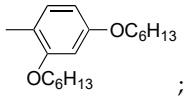 ; $R_{2–10}$: H	CH_3CN	0.1 M $[Bu_4N][ClO_4]$	0.020	[44]
R$_1$: 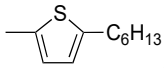 ; **R**$_{2–10}$: H	CH_3CN	0.1 M $[Bu_4N][ClO_4]$	0.090	[44]
R$_1$: 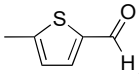 ; **R**$_{2–10}$: H	CH_3CN	0.1 M $[Bu_4N][ClO_4]$	0.130	[44]
R$_1$: 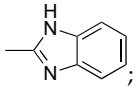 ; **R**$_{2–10}$: H	CH_3CN	0.1 M $[Bu_4N][ClO_4]$	0.075	[45]
R$_1$: 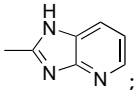 ; **R**$_{2–10}$: H	CH_3CN	0.1 M $[Bu_4N][ClO_4]$	0.085	[45]
R$_{1,10}$: 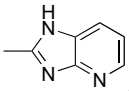 ; **R**$_{2–9}$: H	CH_3CN	0.1 M $[Bu_4N][ClO_4]$	0.205	[45]
R$_{1,10}$: 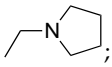 ; **R**$_{2–9}$: H	DCM	0.2 M $[Bu_4N][PF_6]$	0.002	[9]
R$_{1,10}$: 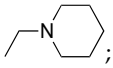 ; **R**$_{2–9}$: H	DCM	0.2 M $[Bu_4N][PF_6]$	−0.001	[9]

Table 2. *Cont.*

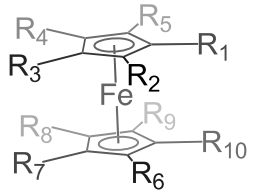	**Solvent**	**Electrolyte**	E_m **vs.** $Fc^{0/+}$ **(V)**	**Ref**
R$_{1,10}$: 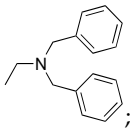 ; **R**$_{2–9}$: H	DCM	0.2 M $[Bu_4N][PF_6]$	−0.001	[9]
R$_1$: 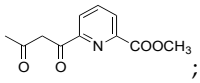 ; **R**$_{2–10}$: H	CH_3CN	0.1 M $[Bu_4N][ClO_4]$	0.366	[45]
R$_1$: 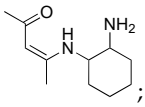 ; **R**$_{2–10}$: H	CH_3CN	0.1 M $[Bu_4N][PF_6]$	0.100	[46]
R$_1$: 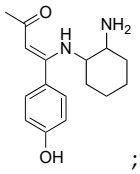 ; **R**$_{2–10}$: H	CH_3CN	0.1 M [BuN]$[PF_6]$	0.120	[46]

3. Ferrocene-Based Electrochemical Sensors Using Oxygen-Containing Host Molecules

Electrochemical molecular recognition refers to the integrated chemical processes by which a redox-responsive receptor molecule recognises and electrochemically senses a guest species [47]. A suitable recognition requires a potential change more significant than the experimental error of the electrochemical technique used. For example, when cyclic voltammetry is used, the mid-point potential change (ΔE_m) should be larger than ±0.005 V. However, this change could be larger than ±0.001 V for potentiometric titrations [12].

Oxygen-containing ferrocene derivatives are vital for sensing alkali and alkaline earth metal ions [48,49]. The mechanism of molecular recognition can be described using a squares scheme where Fc-H, Fc^+-H, G, Fc-HG and Fc^+-HG represent the ferrocene host, ferrocenium host, guest, ferrocene host–guest complex, and ferrocenium host–guest complex, respectively (Scheme 1), where E_{m1} and E_{m2} are the mid-point potentials for the Fc-H/Fc^+-H and Fc-HG/Fc^+-HG redox processes and k_1 and k_2 are the host–guest binding constant for Fc-H and Fc^+-H, respectively [6,47]. The vertical reactions in Scheme 1 represent the guest binding at the host site, which can shift the E_m of the Fc pendant group connected to the host. The horizontal reactions represent the electrochemical electron transfer, where $E_{m1} \neq E_{m2}$ for a suitable electrochemical molecular recognition once the guest ion binds to the host. The larger the shift, the better the electrochemical molecular recognition.

Crown ethers have gained particular interest as hosts within the family of macrocycles. This is due to their unique interwoven structures composed of oxygen and carbon atoms, making them well-suited for binding a wide range of metal ions [50–52]. The first group of cation receptors known for their redox activity that researchers explored consisted of ferrocene crown ether conjugates **1**–**4** [53–56]. These Fc-based electrochemical sensors were developed for alkali cations such as sodium, potassium, caesium and lithium, where the electron-rich crown ether acts as the host centre. Inserting a cation to the crown ether of **1**–**3** results in a substantial E_m shift of Fc to more positive potential values. For example, cyclic voltammograms of 0.2 mM pentaoxa [13] ferrocenophane **1** recorded in CH_2Cl_2/0.1 M $[Bu_4N][PF_6]$ showed a positive E_m shift of 0.17 V after addition of 1 mM $NaClO_4$ [56].

This effect was explained by electrostatic repulsion forces between ferrocenium and the guest Na^+.

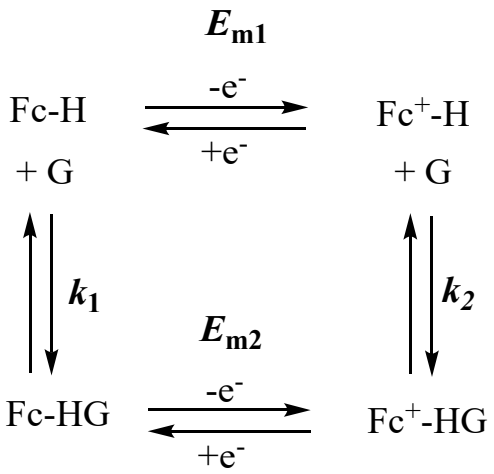

Scheme 1. Square scheme showing coupled electron transfer and guest transfer to and from a ferrocene host molecule.

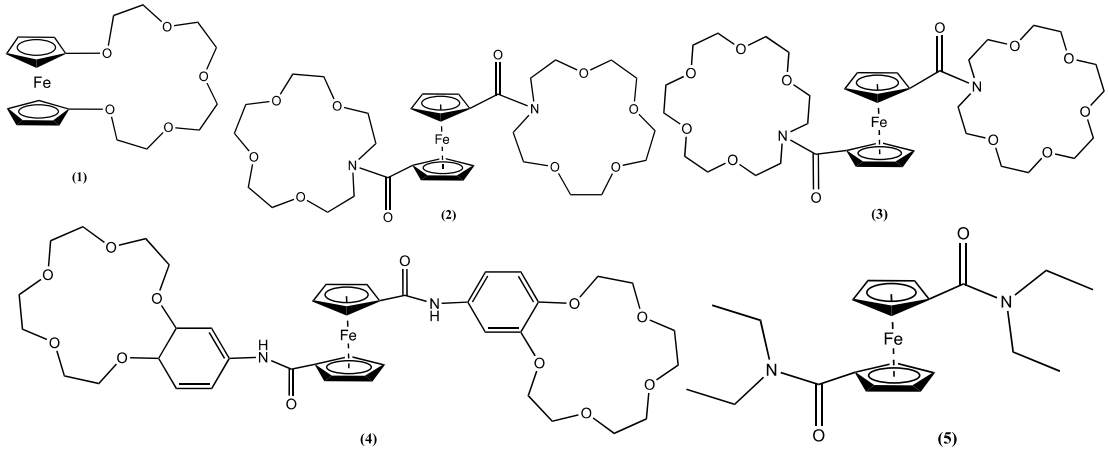

In the case of molecule **2**, the E_m of Fc collected in CH_3CN containing 0.2 M $[Bu_4N][BF_4]$ as the supporting electrolyte showed a significant positive shift of 0.040, 0.020 and 0.070 V after one equivalent of Na^+, K^+ and Li^+ ions were added, respectively. Similar shifts of 0.035, 0.020 and 0.075 V were observed for molecule **3** after adding one equivalent of the respective ions [53]. Nevertheless, the E_m of **4** remained unchanged in the presence of Na^+, K^+ and Li^+ ions, which was argued to be related to the considerable distance between Fc and the host [55]. Notably, the ability to sense alkali cations is not exclusive to the crown ether host. For example, ferrocene amide **5** has a carbonyl oxygen donor, which acts as a host site for Li^+, inducing a positive E_m shift of 0.390 V compared to free **5** [53,57].

Additional investigations into Fc-crown ethers have shown that electronic conjugation can convey a redox reaction when cations bind, even when the binding unit is apart from the Fc reporter group. This can be further explained using molecules **6** and **7** [58]. In molecule **6**, an aza-crown is connected to Fc through an E-stilbene-like linkage. Cyclic voltammetry of **6** in CH_3CN containing 0.2 M $[Bu_4N][BF_4]$ as the supporting electrolyte showed a positive E_m shift of 0.120 V when Mg^{2+} was added. Conversely, for molecule **7**, no discernible cation-induced E_m shift was noticed, which was rationalised as a consequence of the lack of a channel for electronic communication between the host and Fc due to its saturated linker.

Receptor **8**, where an aryl aza-crown is directly bonded to Fc, shows a positive E_m shift of 0.040 V for K^+, 0.090 V for Na^+ and 0.110 V for Mg^{2+} in acetonitrile containing 0.2 M

$[Bu_4N][BF_4]$ as the supporting electrolyte [57]. It was hypothesised that the magnitude of the E_m shift of Fc could be related to the charge/radius ratio of cation guests.

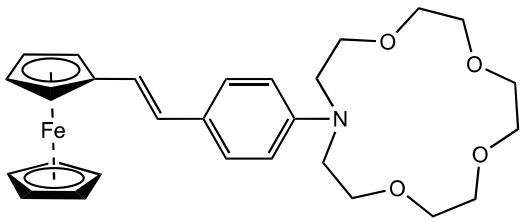

(6)

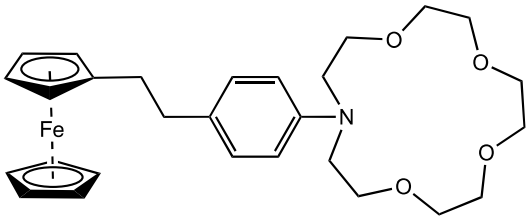

(7)

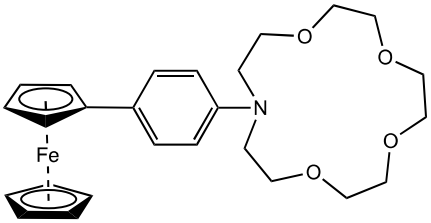

(8)

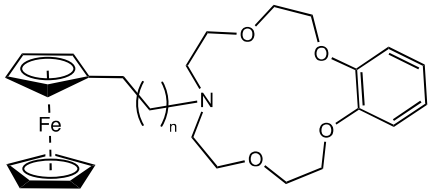

(9)

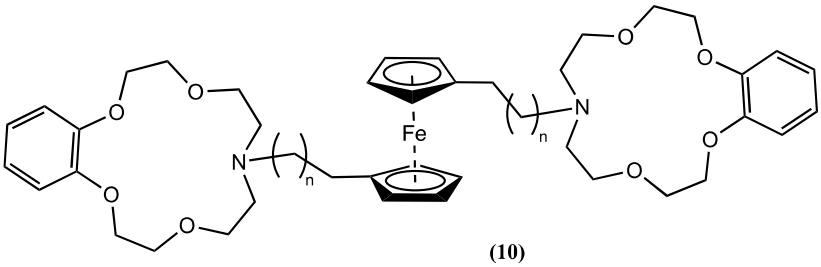

(10)

Two series of ferrocene-linked benzoaza [15] crown-5 host molecules **9** and **10** were synthesised with varying alkyl spacer lengths (n = 0, 1 and 3). Cyclic and square wave voltammetry were employed to investigate the electrochemical behaviour of these ligands in the presence of protons and various metal cations [59]. Significant positive E_m shifts were observed upon cation binding, supporting the Coulombic origin of the through-space interactions. The ΔE_m varied linearly with the inverse of the distance between Fc and the bound cation, in agreement with Coulomb's law. For the optimal condition (n = 0), **9** ΔE_m of 0.163, 0.068 and 0.040 V and **10** ΔE_m of 0.402, 0.292 and 0.159 V for H^+, Mg^{2+} and Ba^{2+} were observed [59].

Fc connected to cryptands is also well-studied as a molecular sensor for cations [60]. Cyclic voltammetry studies showed a positive E_m shift in the presence of alkaline earth and lanthanide cations [61,62]. Molecule **11** showed the most significant E_m positive shift of 0.295 V for Be^{2+} and 0.254 V for Dy^{3+}. These studies have established a broad correlation between the change in redox potential and the charge density of the cationic species.

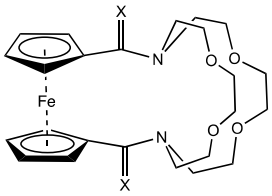

(11) X=O

(12) X=H

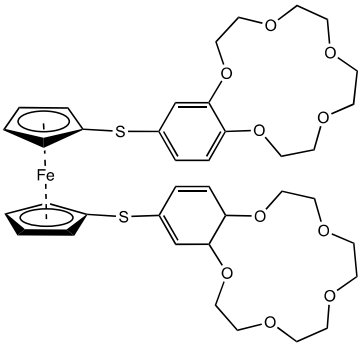

(13)

When alkyl amines replaced the amide groups in **11** as in **12**, a more significant E_m shift was observed after cations binding [63]. For example, the Ca^{2+} binding to **11** and **12** showed a positive E_m shift of 0.155 and 0.275 V, respectively. Also, molecule **12** has an exceptional selectivity for Ag^+, displaying a positive ΔE_m of 0.282 V after Ag^+ binding. It was hypothesised that the flexibility of the alkyl linker greatly influences the coupling between Fc and the cryptand host site.

Interestingly, molecule **13**, which has the Fc connected to two crown ether ligands via sulphur, showed a 0.070 V positive ΔE_m for Na^+ binding and a 0.060 V negative ΔE_m for K^+ ion [48]. The source of this anomalous behaviour is due to conformational changes upon K^+ binding. ^{13}C-NMR and FAB-MS confirmed that the larger size of K^+ causes the receptor molecule to form a 1:1 sandwich complex, whereas the smaller size of the Na^+ ion produces a 1:2 host/guest complex. The 1:2 complex may have the two crown ether units in a *trans*-like configuration with respect to the Fc unit. However, the 1:1 sandwich confirmation forces the two crown ether units to the same side of the Fc, forming a *cis*-like configuration, increasing the Fc instability, and justifying the negative ΔE_m observed.

Molecules **14**, **15** and **16** are examples of Fc linked to varying sizes of cryptands via electron donor oxygen atoms [64]. Upon careful analysis of cyclic voltammetry data for these molecules and their respective alkali and alkaline earth metal complexes in CH_3CN, two trends can be observed: (*a*) the larger the size of the cryptands (**14** < **15** < **16**), the smaller the positive ΔE_m observed; and (*b*) the largest positive ΔE_m was observed for metal ions whose sizes are complementary to the cryptand size. For molecule **14**, the most significant positive ΔE_m of 0.380, 0.360 and 0.305 V was obtained for Ca^{2+}, Sr^{2+} and Ba^{2+}, respectively.

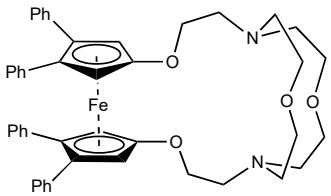

(14)

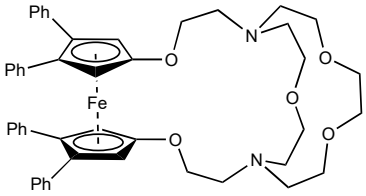

(15)

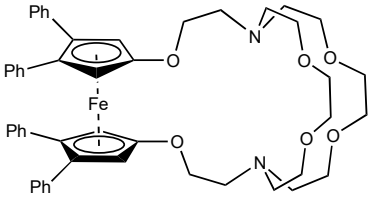

(16)

After complexation with Na^+, **14**, **15** and **16** showed a positive ΔE_m of 0.215, 0.180 and 0.080 V, respectively. This trend supports the theory that the most considerable positive shift was produced by metal ions whose sizes complement the size of the cryptand connected to the Fc unit.

Host units containing di- or tri-aza crown ethers featuring multiple Fc units (**17** and **18**) have been synthesised [65]. Cyclic voltammetry experiments in CH_3CN/0.2 M $[Bu_4N][BF_4]$ showed that the progressive addition of two equivalent K^+ to solutions of **17** or **18** showed a positive ΔE_m of 0.050 and 0.085 V, respectively.

Receptor **19** was synthesised by connecting Fc to an 8-hydroxyquinoline unit [66]. Cyclic voltammograms of **19** in CH_3CN/0.15 M $[Bu_4N][ClO_4]$ show a chemically reversible $Fc^{0/+}$ one-electron process. However, **19** exhibits a negative ΔE_m of 0.149 V after adding one equivalent of Hg^{2+}. This shift was attributed to Hg^{2+}, which enhances the electron density at the Fc centre of **19**. Based on fluorescence data, it was hypothesised that the Hg^{2+} ion binds to the oxygen atoms of the ester group, increasing the intramolecular charge transfer, a phenomenon linked to the influence of heavy atoms [67].

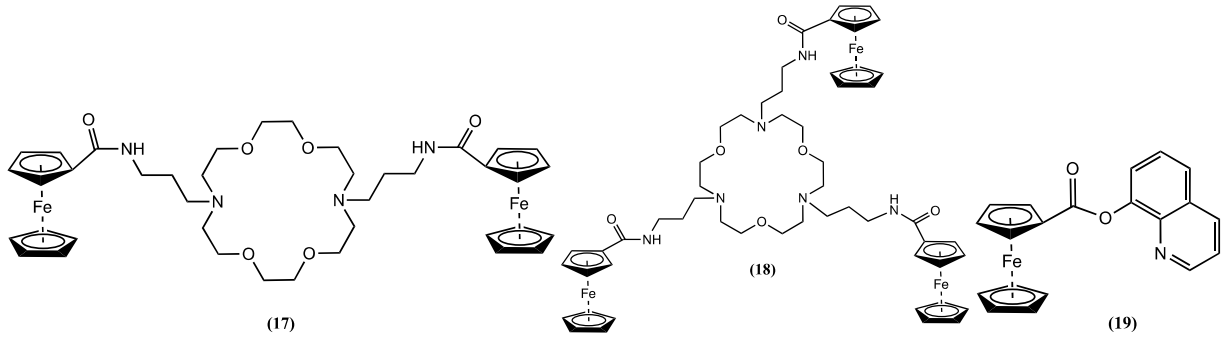

4. Ferrocene-Based Electrochemical Sensors Using Nitrogen-Containing Host Molecules

The interaction between Fc and amines has been the subject of extensive research due to its potential wide application range, including the design of metal ion receptors and sensors [8–10,63,68–72]. However, despite numerous studies, the details of this interaction and the oxidation mechanism of ferrocene-bearing amine compounds have remained elusive until recently, where the oxidation mechanism of N,N-dimethylaminomethylferrocene (**20**, Fc-CH_2-N(CH_3)$_2$), which can be considered as the parent ligand for many Fc receptors presented in this review, was evaluated and the oxidation product identified (Scheme 2) [7].

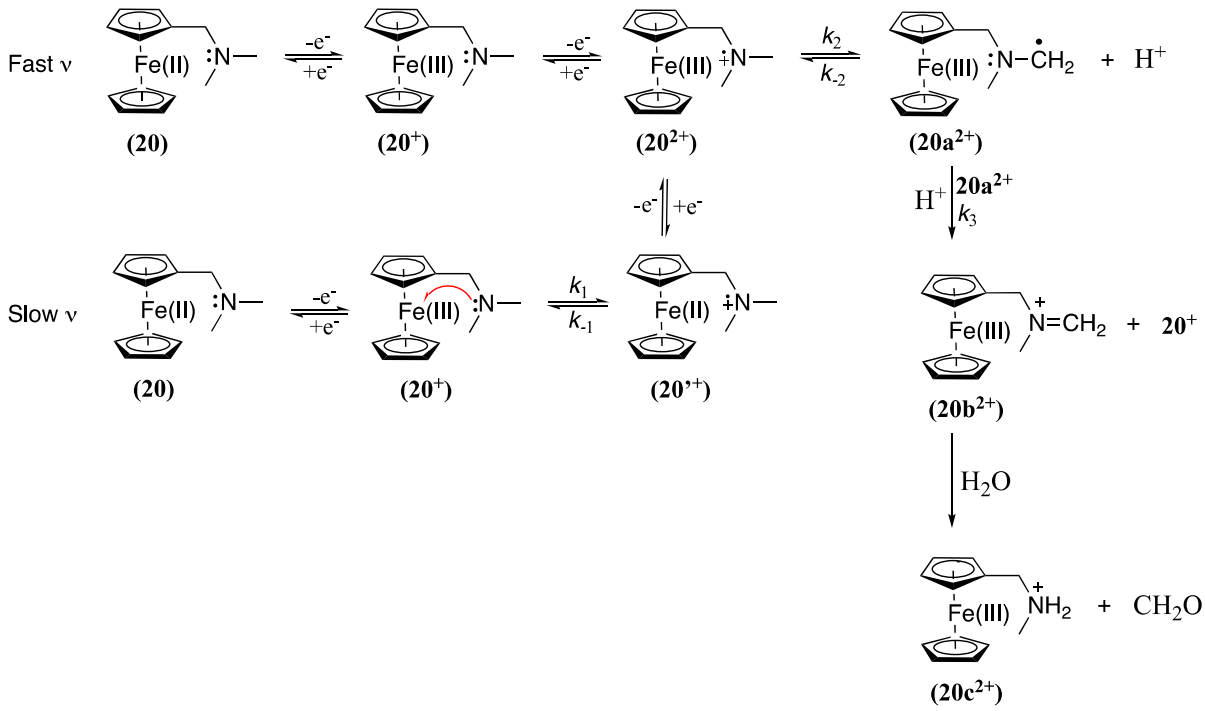

Scheme 2. Schematic representation of the mechanism postulated for the oxidation of **20**.

At fast scan rates (ν), the oxidation process was found to be a simple reversible one-electron oxidation, where the Fc moiety is oxidised to form the ferrocenium cation **20$^+$**. This cation is then further oxidised at more positive potentials to form **20^{2+}**, triggering a reaction sequence that leads to the formation of various intermediate species. Interestingly, the presence of the amine moiety was found to enhance the reactivity of the ferrocenium cation formed on oxidation.

At slow ν, additional steps were observed in the oxidation mechanism. These steps included the formation of terminal methylene radical **20a^{2+}** via two distinct routes: (*i*) via direct oxidation of **20$^+$** when the potential scan is extended to more positive values (as observed at high scan rates) and (*ii*) via an intramolecular electron transfer from a nitrogen

atom to the iron(III) centre (k_1 = 0.05 s^{-1}), effectively regenerating the Fc unit and producing a radical cation designated as **20′⁺**, which can then be further oxidised to form **20²⁺** and subsequently deprotonate to yield **20a²⁺**. A following-up disproportionation reaction regenerates **20⁺** and forms the iminium derivative **20b²⁺**. Water molecules, either existing as contaminants in the organic solvent or introduced during the extraction of the product, may react with **20b²⁺** to produce the secondary ammonium ion **20c²⁺** along with formaldehyde as a side product [7]. Although without product identification, a similar mechanism was postulated for **21**–**26** and related molecules, arriving after oxidation to the corresponding iminium cation [8–10].

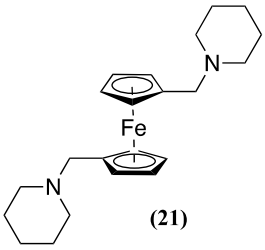

(21)

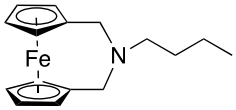

(22)

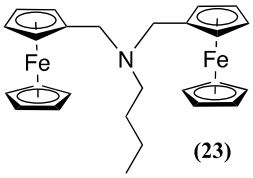

(23)

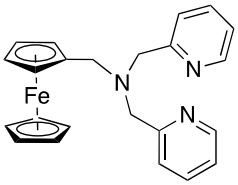

(24)

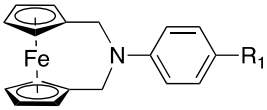

R_1 = Me; *n*-Bu; *t*-Bu; OH

(25)

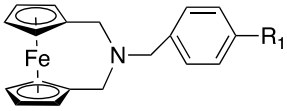

R_1 = Me; CF_3

(26)

The consequence of this finding is that the electrochemical oxidation of the Fc moiety could potentially modify the host affinity for transition metal ions via three distinct mechanisms: (*a*) the development of electrostatic repulsion due to the close spatial proximity of the oxidised Fe(III) centre (as part of the ferrocenium ion) to the binding site; (*b*) the induction of a positive charge on a host nitrogen atom by substitution of a lone electron pair, which diminishes the host ability to complement the target ion; and (*c*) the interaction of the iminium species with water or other nucleophilic molecules leading to the opening of host ring, diminishing the inherent preorganisation of the amine-containing hosts [7]. Consequently, the square scheme described above for oxygen-containing hosts to describe molecular recognition processes may not extend to nitrogen-containing host systems, and caution must be taken when conducting such analyses [47,49].

The Fc bridged cyclam **27** was evaluated by cyclic voltammetry in $CH_3CN/[Bu_4N][PF_6]$ and showed a significant positive ΔE_m of 0.360 V for Co^{2+}, 0.380 V for Ni^{2+}, 0.410 V for Cu^{2+}, and 0.470 V for Zn^{2+} [73]. The significant positive E_m shift in the presence of metal ions could be a through-space electrostatic interaction, which causes a substantial perturbation of the E_m of Fc. Molecule **27** was also used as a selective sensor for Cu^{2+}, which showed an ΔE_m of 0.210 V in the presence of Cu^{2+} in 70:30 1,4-dioxane:0.1 M KNO_3 aqueous solution (pH 5.0). Interestingly, the E_m was not affected by the presence of Ni^{2+}, Zn^{2+}, Cd^{2+}, Hg^{2+} and Pb^{2+} ions [74].

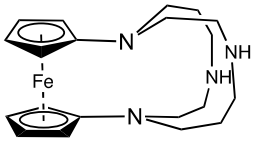

(27)

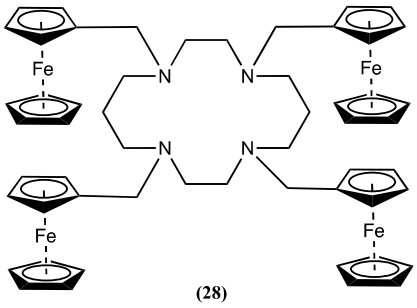

(28)

The electrochemical behaviour of **28** in 1:1 DCM:MeOH/$[Bu_4N][PF_6]$ was studied in the absence and presence of Cu^{2+} [75]. The addition of Cu^{2+} resulted in a positive E_m shift of 0.094 V. However, no E_m changes were observed when **28** was in contact with Ni^{2+}, which was hypothesised to be related to the slow complexation kinetics.

Acyclic receptor molecules **29**–**31** were synthesised, and their interaction with transition metals was evaluated [76]. It was observed that the added metal ions may directly coordinate with host molecules or protonate them by acting as an acid. For example, **29** coordinates with Ni^{2+} and Cu^{2+}, generating a positive E_m shift of 0.058 and 0.098 V, respectively. Instead, the addition of Zn^{2+} undergoes a protonation pathway of the receptor, causing a positive E_m shift of 0.162 V. In contrast, **30** exclusively follows the protonation pathway due to the large bite angle of the host group. Adding Ni^{2+}, Cu^{2+} and Ca^{2+} to **30** showed a positive E_m shift of 0.175, 0.169 and 0.160 V, respectively. Meanwhile, the pyridine nitrogen atom in **31** participates in the coordination of metal ions. Its interaction with Ni^{2+}, Cu^{2+} and Zn^{2+} resulted in a positive E_m shift of 0.115, 0.105 and 0.075 V, respectively [76].

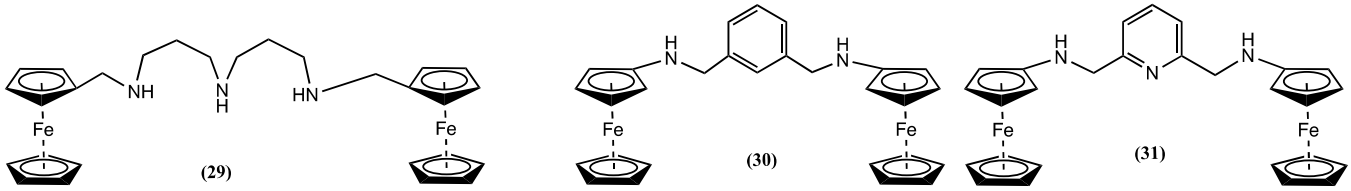

The electrochemical sensor **32** forms a square–planar complex with Ni^{2+}, showing a slight positive E_m shift of 0.025 V in an aqueous 0.1 M $NaClO_4$ solution [77]. However, due to the presence of two electron-deficient amide nitrogen atoms in **33**, the dioxotetraamino host shows a poor tendency towards complexation [77]. This behaviour changes when Ni^{2+} is complexed under basic conditions, where nitrogen deprotonations result in a double negative charge on the ring system of **33**, forming a stable four-coordinated system that generates a negative E_m shift of 0.042 V [11,77].

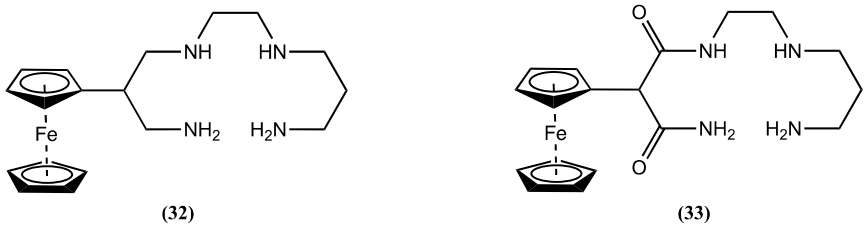

Recently, we synthesised cyclen and cyclam macrocycles bearing ferrocene pendants and investigated their ability to work as electrochemical sensors for transitional metal cations [7]. The cyclic voltammograms **34** in 1:4 CH_2Cl_2:CH_3CN/0.1 M $[Bu_4N][PF_6]$ showed upon addition of Ni^{2+}, Cd^{2+}, Zn^{2+}, Cu^{2+} and Co^{2+} ions a positive E_m shift of 0.054, 0.057, 0.078, 0.100 and 0.120 V, respectively. Similarly, when Zn^{2+} coordinates with molecule **35**, a positive E_m shift of 0.098 V was observed.

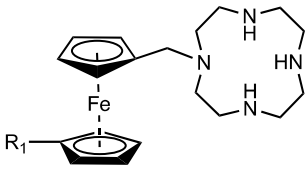

(34) R_1=H
(35) R_1=CH_2OH

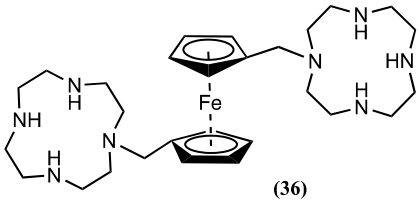

(36)

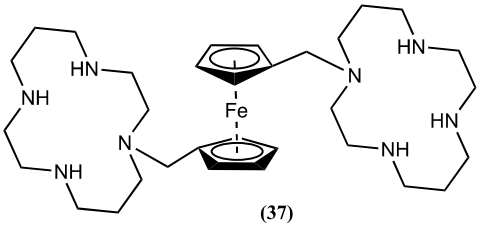

(37)

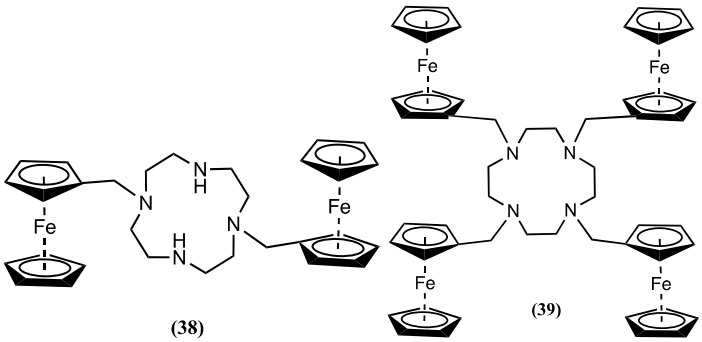

(38) **(39)**

The addition of Ni^{2+}, Cd^{2+}, Zn^{2+}, Cu^{2+} and Co^{2+} ions to a solution of **36** in 1:4 CH_2Cl_2:CH_3CN/0.1 M $[Bu_4N][PF_6]$ generates a positive E_m shift of 0.148, 0.160, 0.203, 0.240 and 0.280 V, respectively. Similarly, cyclic voltammograms of **37** showed a comparable response in the presence of the mentioned ions, generating a positive E_m shift of 0.184 V for Ni^{2+}, 0.179 V for Cd^{2+}, 0.183 V for Zn^{2+}, 0.239 V for Cu^{2+} and 0.259 V for Co^{2+}.

The cyclic voltammetric behaviour of **38**, where two Fc units are linked via the cyclen host group, was studied in detail before and after complexation with 3*d* and 4*d* transition metal cations. The complexation reaction between **38** and Ni^{2+}, Cd^{2+}, Zn^{2+}, Cu^{2+} and Co^{2+} ions resulted in a positive E_m shift of 0.064, 0.060, 0.088, 0.111 and 0.132 V, respectively. Similarly, **39**, where four Fc units are attached to the cyclen host group, was also investigated. Adding Cd^{2+}, Zn^{2+}, Cu^{2+} and Co^{2+} to **39** resulted in a positive ΔE_m of 0.053, 0.047, 0.078 and 0.022 V, respectively. However, no response was observed after the addition of Ni^{2+} ions.

Based on electrochemical data, the charge density of transition metal ions can be correlated with the ΔE_m observed, except for Ni^{2+}. The magnitude of the E_m shift follows the order **36** ≈ **37** >> **34** ≈ **35** ≈ **38** > **39** and depends on the number of macrocycles linked to Fc. Nonetheless, no significant change in E_m can be obtained by increasing the number of Fc groups attached to a guest macrocycle [7].

The redox behaviour of **40**–**44** was studied in CH_3CN/0.1 M $[Bu_4N][ClO_4]$ [45]. Receptor **40** showed a positive E_m shift of 0.250 V after adding Pb^{2+}, Zn^{2+} or Hg^{2+} ions. However, **41** shows a maximum response after adding one equivalent of Pb^{2+}, presenting a positive E_m shift of 0.150 V. Similarly, **41** showed a positive ΔE_m of 0.090 and 0.120 V for Zn^{2+} and Hg^{2+} ions. This shift was very specific, and the cyclic voltammogram of **41** was not affected by adding large quantities of Li^+, Na^+, K^+, Ca^{2+}, Mg^{2+}, Ni^{2+} and Cd^{2+} ions. Likewise, **42** showed a positive E_m shift of 0.120 V in the presence of Pb^{2+}. Consequently, the positive E_m shift for the monosubstituted Fc after complexing with Pb^{2+} is **42** < **41** < **40**.

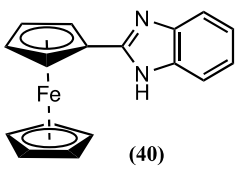

(40)

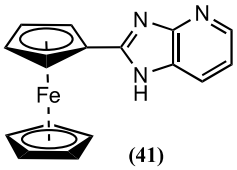

(41)

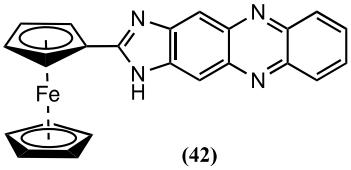

(42)

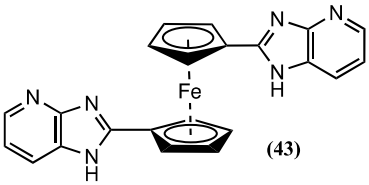

(43)

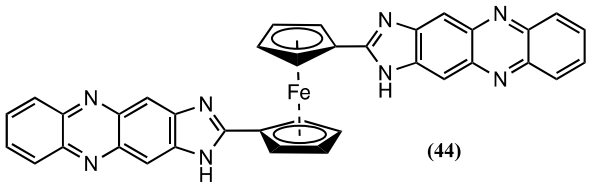

(44)

Receptors **43** and **44** also display selectivity for Pb^{2+} and Zn^{2+}. Molecule **43** showed a positive E_m shift of 0.180 and 0.190 V upon adding one equivalent of Pb^{2+} and Zn^{2+}, respectively. A comparable trend was also found for **44**, which undergoes a positive ΔE_m of 0.110 and 0.170 V for the same cations. The ΔE_m observed for Zn^{2+} starkly contrasts observations made with the related molecules **41** and **42**, which is in agreement with previous works, where the complexation of Zn^{2+} ions to 1,1′-disubstituted ferrocene resulted in a large positive E_m shift with respect to 1-monosubstituted ferrocene [7,78]. The receptor **45**, which differs from **40** by a methyl group in the benzimidazole ring, was electrochemically studied in CH_3CN/0.1 M $[Bu_4N][ClO_4]$ [79]. It displayed specific sensing capability for Sn^{2+} ions, showing a positive E_m shift of 0.230 V after adding one equivalent of Sn^{2+} ions. Similarly, the ability of **46** and **47** to sense different metal ions was assessed in 1:1 CH_3CN:DCM/0.01M $[Bu_4N][PF_6]$ [80]. In the presence of Hg^{2+} and Pb^{2+}, **46** showed a positive E_m shift of 0.050 and 0.060 V, whereas **47** showed a positive ΔE_m of 0.150 V for Hg^{2+} and 0.040 V for Pb^{2+} after complexation. Notably, the presence of a 3-pyridyl unit in the sensors, regardless of location, significantly enhanced their ability to detect Hg^{2+} selectively and sensitively. It is worth noting that the 3-pyridyl unit did not directly coordinate with metal ions despite its influence on the improved performance.

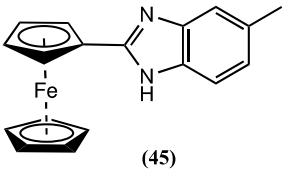

(45)

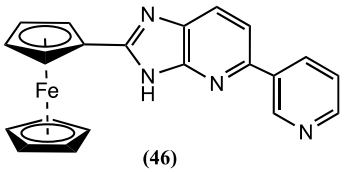

(46)

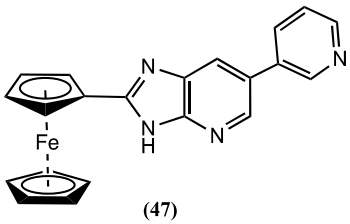

(47)

Sensors **48–50** were synthesised by connecting a Fc unit to a pyridyl moiety using a β-diketone bridge [81]. The complexing properties of these sensors towards Zn^{2+}, Hg^{2+}, Co^{2+}, Cu^{2+}, Mn^{2+}, Cd^{2+} and Ni^{2+} ions were investigated in ethanol/0.1 M $LiClO_4$. The largest positive E_m shifts were obtained after adding Cu^{2+} and Cd^{2+} to a solution of **48,** showing ΔE_m = 0.072 and 0.067 V, respectively. Meanwhile, positive E_m shifts of 0.102 V for Cu^{2+} and 0.109 V for Mn^{2+} were reported for **49**.

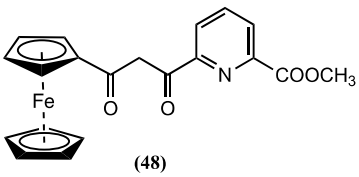

(48)

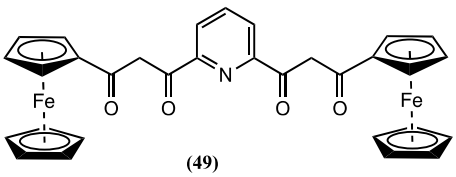

(49)

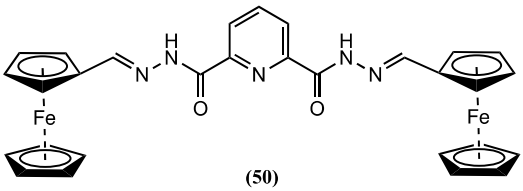

(50)

Similarly, **50** results in a positive E_m shift of 0.053 V for Hg^{2+} and 0.054 V for Mn^{2+} ions. Yet, the receptors **49** and **50** exhibit significantly lower redox potential shifts when treated with Zn^{2+}, Hg^{2+}, Co^{2+}, Cd^{2+} and Ni^{2+} ions.

Meanwhile, naphthalimide was connected to a ferrocenyl–chalcone group using a triazole linker, and the electrochemical properties of the resulting molecule **51** to sense Cu^{2+}

ion in CH_3CN/0.01 M $[Bu_4N][ClO_4]$ was evaluated [82]. A 0.5 mM **51** solution showed a positive ΔE_m of 0.020 V upon adding 30 μM Cu^{2+} ion.

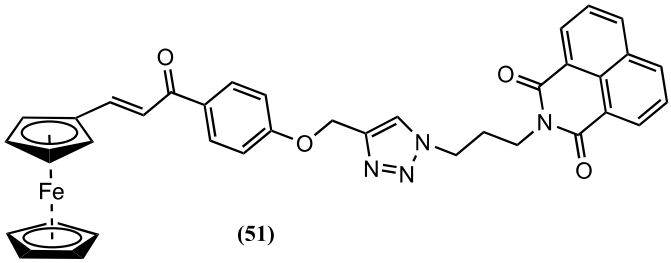

(51)

Two receptors, **52** and **53**, which incorporate Fc and rhodamine-containing triazole, were synthesised, and their electrochemical properties to sense metal cations in CH_3CN/0.1 M $[Bu_4N][ClO_4]$ were explored [83]. The E_m of these receptors was not affected by the presence of Na^+, Mg^{2+}, K^+, Ca^{2+}, Cr^{2+}, Mn^{2+}, Fe^{2+}, Co^{2+}, Ni^{2+}, Cu^{2+}, Zn^{2+}, Pb^{2+}, Cd^{2+} and Tl^+ ions. However, introducing one equivalent of Hg^{2+} led to a positive E_m shift of 0.200 and 0.250 V for **52** and **53**, respectively. NMR studies of the **52**-Hg^{2+} complex indicated that Hg^{2+} ions coordinate with the nitrogen atoms of the triazole ring, the imine, the oxygen atom linked directly to the methylene, and the amide carbonyl group [83]. A similar molecule, **54**, shows a negative ΔE_m of 0.050 V upon adding one equivalent of Hg^{2+}. HR-MS and FT-IR studies suggest that the spirolactam ring undergoes an opening process when Hg^{2+} binds to **54**. Consequently, it is believed that the pyridine nitrogen atom and two amide oxygen atoms of **54** potentially form coordination bonds with Hg^{2+}, creating a chelating complex in conjunction with a solvent molecule [83].

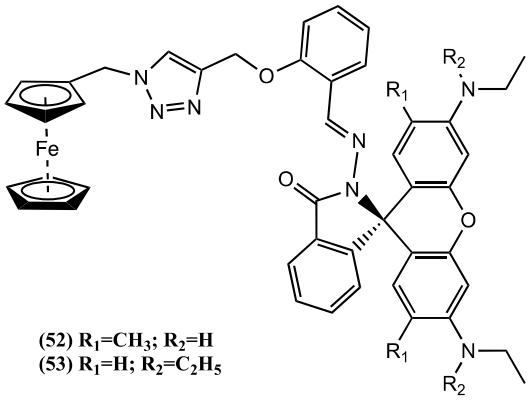

(52) R_1=CH_3; R_2=H
(53) R_1=H; R_2=C_2H_5

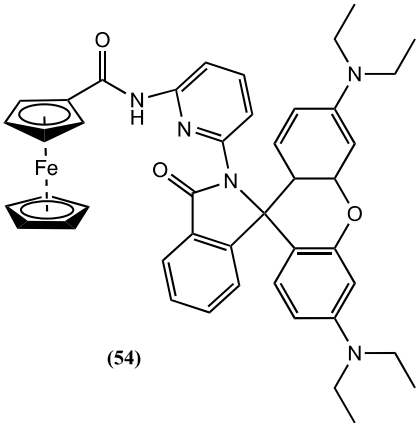

(54)

The strained asymmetric sensor **55** was synthesised and electrochemically evaluated in DCM/0.1 M $[Bu_4N][ClO_4]$ [84]. The cyclic voltammograms revealed two closely spaced, reversible oxidation peaks at 0.510 and 0.740 V vs. SCE. The initial reversible oxidation process was assigned to the oxidation of the single-substituted Fc unit and the second to the oxidation of the 1,1′-disubstituted Fc unit. While the addition of Ca^{2+} ions did not cause any E_m changes, a noticeable change was observed upon introducing one equivalent of Mg^{2+} ions, where a positive E_m shift of 0.340 V was observed in the second peak. Meanwhile, a small positive ΔE_m of 0.030 V was reported for the first peak. This sensor could distinguish between Mg^{2+} and Ca^{2+} ions without being affected by excess amounts of Li^+, Na^+, and K^+ ions [84].

Molecule **56** was studied in 4:1 DCM:CH_3CN/0.1 M $[Bu_4N][PF_6]$ [85]. The cyclic voltammogram displayed two electrochemically reversible one-electron peaks at $E_m = -0.060$ and 0.460 V vs. $Fc^{0/+}$. Adding increasing quantities of Zn^{2+} into a solution of **56** led to the partial disappearance of the peak at -0.060 V and the appearance of a new peak at 0.020 V. However, there were no noticeable E_m changes in the second peak of the receptor. Unsymmetrical related molecules **57–59** were evaluated with respect to a range of cations, including Li^+, Na^+,

K^+, Ca^{2+}, Mg^{2+}, Ni^{2+}, Cd^{2+}, Zn^{2+}, Pb^{2+}, Hg^{2+} and Cu^{2+} in 4:1 or 3:2 CH_3CN:DCM/0.1 M $[Bu_4N][PF_6]$ [86]. Each free receptor displayed two reversible one-electron redox processes. Compound **57** shows these processes at 0.050 and 0.250 V vs. $Fc^{0/+}$, **58** at 0.050 and 0.310 V and **59** at 0.030 and 0.240 V. In all three cases, the initial oxidation process pertains to the Fc unit with a single substitution. The second oxidation wave is associated with the Fc unit bearing two substitutions.

Adding Pb^{2+} ions to **57** generates a positive E_m shift of 0.050 V for the first process and a negative E_m shift of 0.150 V for the second. A similar situation was observed after adding Zn^{2+}, with a positive E_m shift of 0.060 V for the first process and a negative ΔE_m of 0.140 V for the second. In the case of **58**, the second process presented a positive E_m shift of 0.050 V for Cd^{2+}, 0.130 V for Ni^{2+}, 0.150 V for Pb^{2+} and 0.140 V for Zn^{2+}. Nevertheless, adding Pb^{2+} ions to **59** generates a positive E_m shift of 0.040 V for the first process and a negative ΔE_m of 0.160 V for the second. Similarly, adding Zn^{2+} causes a positive E_m shift of 0.010 V for the first process and a negative ΔE_m of 0.200 V for the second one [86]. As a result of this experiment, adding Pb^{2+} and Zn^{2+} to **57** and **59** resulted in a concurrent positive shift of the lower E_m and a negative shift of the higher E_m. This causes a single wave to appear in the cyclic voltammograms of the final complex due to the overlapping of the two oxidation processes part of the receptors. Nevertheless, the most noteworthy change occurs in the higher oxidation process when Ni^{2+}, Cd^{2+}, Zn^{2+} and Pb^{2+} are added to probe **58**. This process experiences a reduction in intensity until it completely disappears when one equivalent of the metal ion is present. Concurrently, the lower oxidation process remains unchanged. This observation implies that the triazole group plays a minor role in interacting with metal cations during complexation. As a result, the primary binding process is likely concentrated in the imine arm of the various receptors, with particular emphasis on receptor **58**, which incorporates an additional quinoline ring [86].

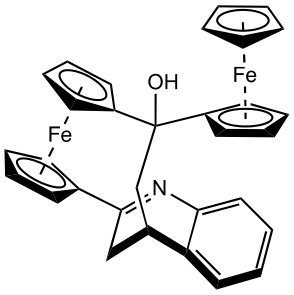

(55)

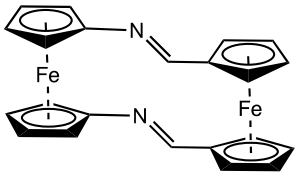

(56)

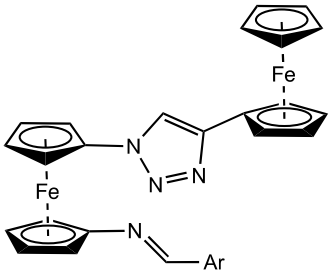

Ar=

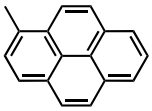

(57)

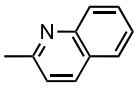

(58)

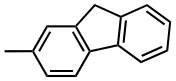

(59)

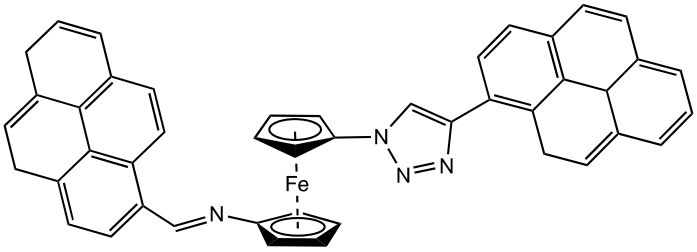

(60)

A related molecule **60,** containing one Fc unit, was studied in 4:1 CH_3CN:DCM/0.1 M $[Bu_4N][PF_6]$ [87]. Free **60** showed a one-electron reversible process at 0.195 V vs. $Fc^{0/+}$ IRRS. A new reversible process at 0.045 and 0.200 V more positive potential values was observed after adding Zn^{2+} and Pb^{2+}, respectively. Notably, the cyclic voltammetric behaviour of **60** is not affected by adding other ions, such as Li^+, Na^+, K^+, Mg^{2+}, Ca^{2+}, Ni^{2+}, Cu^{2+}, Cd^{2+} and Hg^{2+}.

The receptor **61** was studied in CH_3CN containing 0.1 M $[Bu_4N][PF_6]$ as the supporting electrolyte. Meanwhile, receptor **62** was evaluated in 9:1 CH_2Cl_2:DMF/0.1 M $[Bu_4N][PF_6]$ [88]. Each free receptor displayed a characteristic reversible one-electron redox process, with E_m= 0.575 V for **61** and E_m = 0.470 V vs. $DmFc^{0/+}$ IRRS for **62**. The E_m of **61** shifted in the positive direction by 0.333, 0.282, 0.224, 0.274 and 0.361 V after adding Zn^{2+}, Pb^{2+}, Ni^{2+}, Cd^{2+} and Hg^{2+}, respectively. In contrast, **62** showed a positive ΔE_m = 0.260 V in the presence of Hg^{2+}. Based on NMR and theoretical studies, it was postulated that the coordination of metal ions to receptor **61** occurs via imine and quinoline nitrogen. Similarly, the ferrocene appended phenolic hydroxyl Schiff base **63** was studied in MeOH/0.1 M $[Bu_4N][ClO_4]$ [89]. Adding Al^{3+}, Cr^{3+} or Fe^{3+} to a solution of **63** resulted in a positive shift in the E_m of 0.028, 0.044 and 0.015 V, respectively.

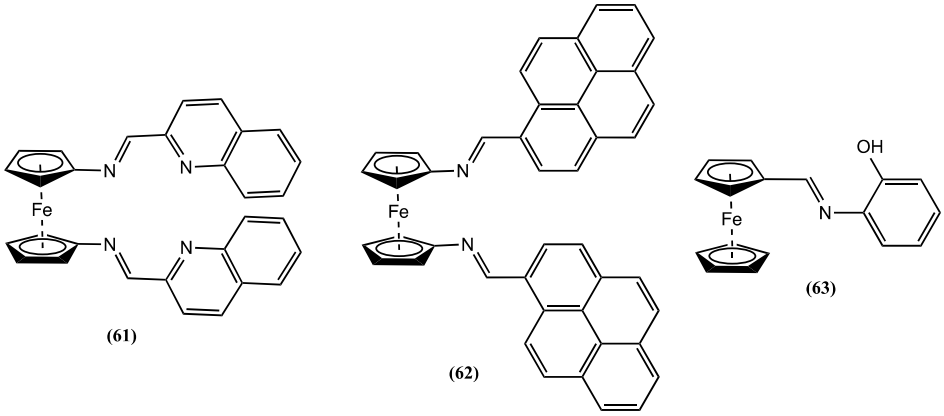

Cyclic voltammetric experiments of **64** and **65** were performed in 3:7 CH_3CN:H_2O/0.1 M $[Bu_4N][ClO_4]$ solutions. Their ability to detect the presence of Li^+, Na^+, K^+, Ca^{2+}, Mg^{2+}, Cr^{3+}, Zn^{2+}, Fe^{3+}, Ni^{2+}, Co^{2+}, Cu^{2+}, Cd^{2+}, Hg^{2+} and Pb^{2+} ions was evaluated [90]. Both receptors **64** and **65** displayed a reversible one-electron oxidation process, in which E_m are not perturbed by the presence of the mentioned ions, except for Hg^{2+}, where the addition of one equivalent of this ion generates a positive E_m shift of 0.076 and 0.043 V for **64** and **65**, respectively. No Hg^{2+} ion sensing ability improvement is obtained with **66** or **67**. Receptor **66** can be seen as the dimeric version of **64**, and its E_m shifts by 0.078 V in the positive direction after adding Hg^{2+} [91]. However, the E_m of receptor **67** shifts by 0.033 V when exposed to Hg^{2+} ions [92]. Based on ^{1}H-NMR titration analysis, it was inferred that the Hg^{2+} binds to the triazole ring nitrogen atom and the oxygen atom in the OCH_2 bridging group [91].

Receptors **68** and **69** containing monosubstituted Fc pendants and **70** and **71** containing disubstituted Fc pendants have been synthesised and electrochemically studied in CH_3CN containing 0.1 M $[Bu_4N][PF_6]$ as the supporting electrolyte [93]. The addition of Ni^{2+}, Hg^{2+} and Pb^{2+} to **68** resulted in the appearance of a new oxidation process, showing a positive ΔE_m of 0.053, 0.025 and 0.014 V, respectively. In contrast, **69** showed a positive E_m shift of 0.072 V upon adding an Hg^{2+} ion. A similar response was observed with the related receptor **70**, which showed a reversible two-electron process at E_m = 0.544 V vs. $DmFc^{0/+}$ for the terminal Fc groups and a reversible one-electron process at E_m = 0.953 V vs. $DmFc^{0/+}$ related to the disubstituted central Fc group [93]. Adding Zn^{2+}, Hg^{2+} and Pb^{2+} to **70** produced a negligible E_m shift for the terminal Fc groups but an E_m shift of 0.032, 0.076 and 0.022 V, respectively, for the central Fc group. In the case of **71**, only the Hg^{2+} ion produced a significant response, showing a positive E_m shift of 0.035 V after adding one equivalent of the mentioned ion.

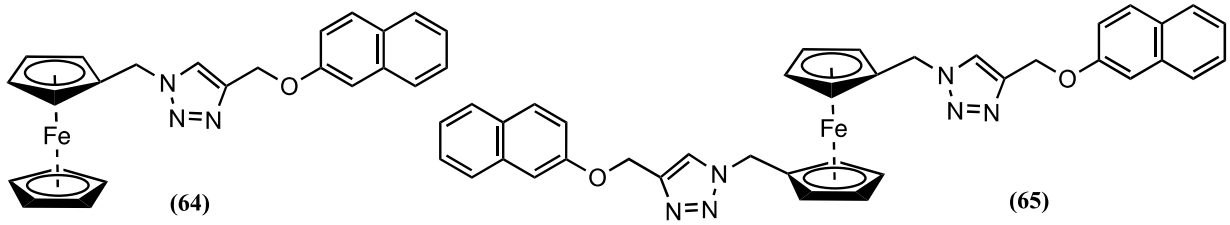

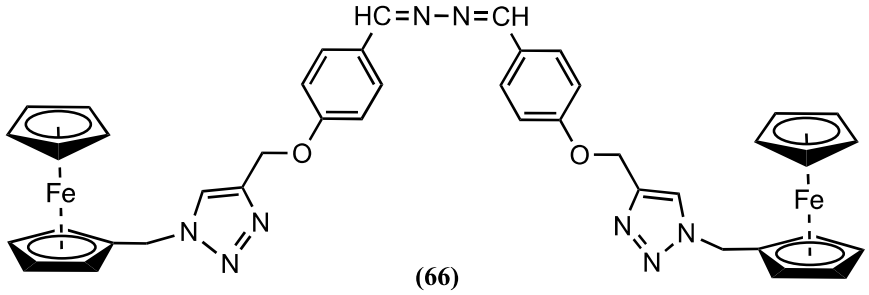

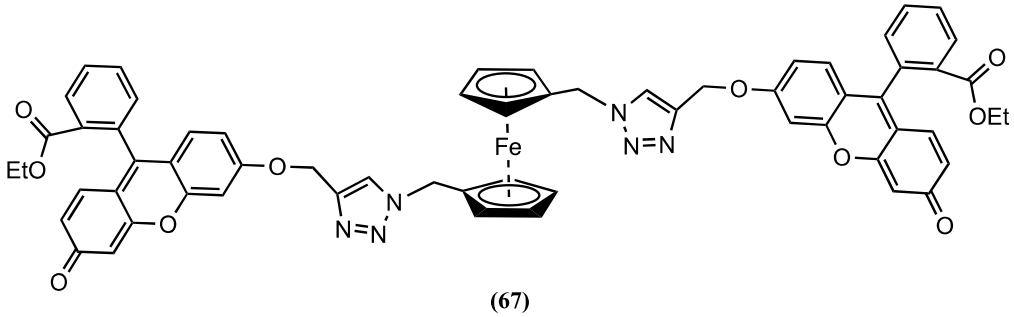

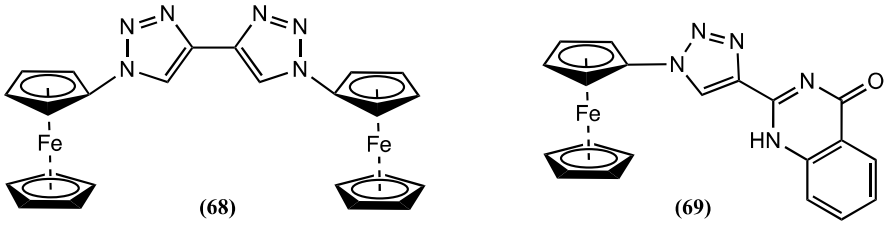

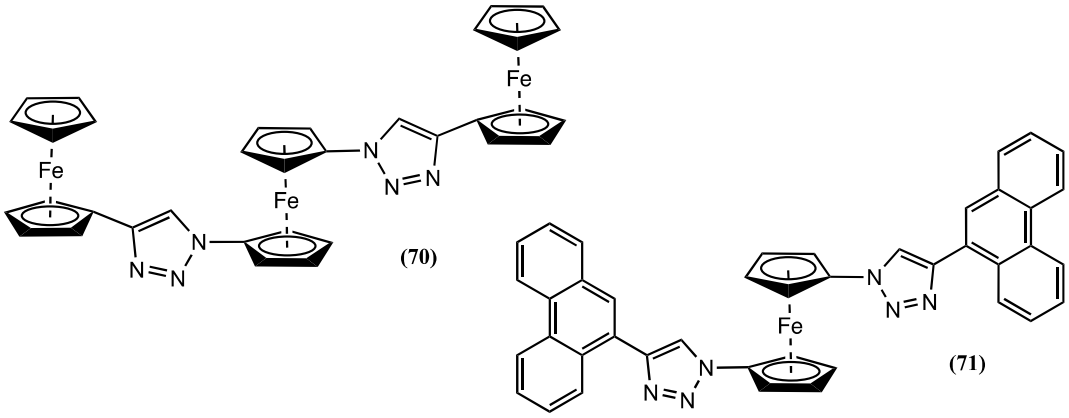

Cyclic voltammetry of **72** in CH_3CN containing 0.01M $[Bu_4N][ClO_4]$ as the supporting electrolyte showed a one-electron reversible process, in which E_m shifted positively by 0.065 V after the addition of Fe^{3+} ions to the solution [94]. Meanwhile, Ferrocene quinazolines **73** was studied in 1:1 ethanol:H_2O/0.1M $[Bu_4N][ClO_4]$ [95]. The introduction of Hg^{2+} to this solution caused the appearance of a new irreversible process at 0.136 V more positive to the E_m of **73**. Similarly, adding Pb^{2+} to a solution of **73** resulted in a negative E_m shift of 0.025 V [95].

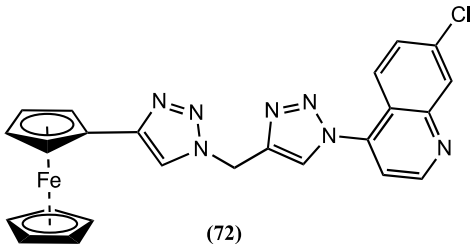

(72)

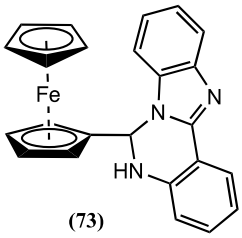

(73)

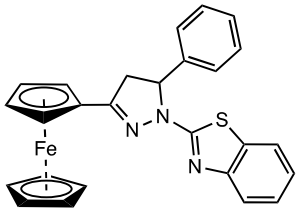

(74)

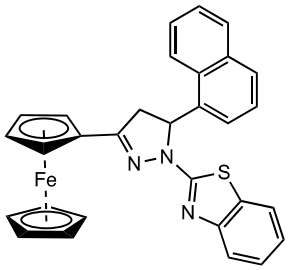

(75)

The interaction of **74** and **75** with various metal ions was systematically studied in acetonitrile using cyclic voltammetry and differential pulse voltammetry [96]. The addition of Hg^{2+} ions to this solution produces the appearance of a new process at 0.078 and 0.100 V more positive potentials with the consequent disappearance of the process related to the free **74** and **75** receptors, respectively. Conversely, when one equivalent of Cu^{2+} ions was introduced to the receptor solutions, a single process was observed, showing a positive E_m shift of 0.042 V for receptor **74** and 0.048 V for receptor **75**. The ^{1}H NMR analysis of the **74**-Hg^{2+} complex showed that the ion interacts with the nitrogen atoms in 1H-pyrazoline and 2-benzothiazole. This finding is supported by theoretical computations conducted using density functional theory [96].

Sensor **76** was studied in a CH_3OH/H_2O solution containing 0.1M KNO_3 as the supporting electrolyte [97]. The addition of 0.5 equivalents of Cu^{2+} to this solution resulted in the appearance of two reversible one-electron redox processes. The first one was related to the redox process of the free **76**, and the second, appearing at 0.125 V with more positive potentials, was assigned to the **76**-Cu^{2+} complex. When one equivalent of Cu^{2+} was introduced, the redox process of the free **76** disappeared. Interestingly, the E_m of **76** is not affected by the presence of other metal ions, such as Mg^{2+}, Ni^{2+}, Zn^{2+}, Pb^{2+} and Cd^{2+}.

Receptor **77** was investigated in a 7:3 dioxane/water containing $[Bu_4N][ClO_4]$ as the supporting electrolyte, revealing its pH-dependent behaviour, shifting E_m towards more positive potentials as the pH decreased from 12 to 5 [98]. Additionally, the presence of Mn^{2+}, Co^{2+}, Ni^{2+}, Cu^{2+} and Zn^{2+} shifted the E_m of **77** in the positive potential direction by 0.046 V for Cu^{2+}, 0.020 V for Co^{2+}, 0.015 V for Mn^{2+}, 0.013 V for Ni^{2+} and 0.009 V for Zn^{2+} [98].

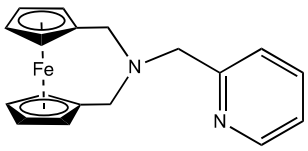

(76)

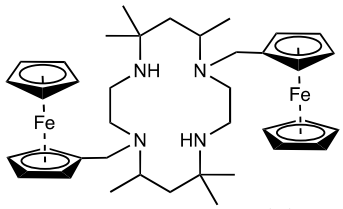

(77)

5. Conclusions

Significant advances have been made in developing Fc receptors capable of selectively sensing metal cations. This review presented a detailed discussion of how oxygen and

nitrogen-containing macromolecular receptors featuring Fc moiety can initially form bonds and then exhibit shifts in redox potentials in response to positively charged guest molecules. This interaction occurs via electrostatic perturbation across space or linked conjugated bonds connecting the Fc unit to the metal cation host binding unit. The general factors that affect the magnitude of the redox potential shift upon binding of the cations to the guest site depend on (*i*) the complementarity between the ferrocene-containing host and guest cation, encompassing the thermodynamics and kinetics of their binding interactions, (*ii*) the charge-to-size ratio of the metal cation, (*iii*) the closeness of the binding site to the redox active Fc, (*iv*) the type of chemical bond that connects the host to the Fc pendant and (*v*) the nature of the solvent used during the experiment. This review also examined the complexity involved in the interplay between electron transfer and molecular recognition where hosts with amine functionalities such as cyclen and cyclam are utilised.

So far, most cation recognition has been conducted in organic solvents. This presents a significant challenge when using these ferrocene-based molecular receptors in aqueous solvents, a requirement for ion recognition in biological systems. To add to the complexity, competing redox active molecules against ferrocene probes might also influence the sensor's specificity. These challenges could open an excellent opportunity to enhance the ability of receptors to selectively bind cation guests, particularly in intricate aqueous environments and integrate them into electrochemical device platforms.

Author Contributions: Conceptualisation, A.K.V.M. and A.A.J.T.; methodology, A.K.V.M. and A.A.J.T.; software, A.K.V.M. and A.A.J.T.; validation, A.K.V.M. and A.A.J.T.; formal analysis, A.K.V.M. and A.A.J.T.; investigation, A.K.V.M. and A.A.J.T.; resources, A.K.V.M. and A.A.J.T.; data curation, A.K.V.M. and A.A.J.T.; writing—original draft preparation, A.K.V.M. and A.A.J.T.; writing—review and editing, A.K.V.M. and A.A.J.T.; visualisation, A.K.V.M. and A.A.J.T.; supervision, A.K.V.M. and A.A.J.T.; project administration, A.K.V.M. and A.A.J.T.; funding acquisition, A.K.V.M. and A.A.J.T. All authors have read and agreed to the published version of the manuscript.

Funding: This research received no external funding.

Data Availability Statement: Not applicable.

Conflicts of Interest: The authors declare no conflict of interest.

References

1. Lehn, J.M. *Supramolecular Chemistry*; Wiley-VCH: New York, NY, USA, 1995; pp. I–X.
2. Zanello, P. *Inorganic Electrochemistry: Theory, Practice and Application*; The Royal Society of Chemistry: Cambridge, UK, 2003.
3. Molina, P.; Tárraga, A.; Caballero, A. Ferrocene-Based Small Molecules for Multichannel Molecular Recognition of Cations and Anions. *Eur. J. Inorg. Chem.* **2008**, *2008*, 3401–3417. [CrossRef]
4. Togni, A.; Hayashi, T. (Eds.) *Ferrocenes: Homogeneous Catalysis, Organic Synthesis, Materials Science*; VCH: New York, NY, USA, 1995.
5. Casado, C.M.; Alonso, B.; García-Armada, M.P. 7.02—Ferrocenes and Other Sandwich Complexes of Iron. In *Comprehensive Organometallic Chemistry IV*; Parkin, G., Meyer, K., O'hare, D., Eds.; Elsevier: Oxford, UK, 2022; pp. 3–45.
6. Stepnicka, P. (Ed.) *Ferrocenes: Ligands, Materials and Biomolecules*; John Wiley & Sons, Ltd.: Chichester, UK, 2008.
7. Torriero, A.A.J.; Zeng, Z.; Mruthunjaya, A.K.V.; Bond, A.M. Electrochemical Properties of Cyclen and Cyclam Macrocycles Bearing Ferrocenyl Pendants and Their Transition Metal Complexes. *J. Electroanal. Chem.* **2023**, *945*, 117687. [CrossRef]
8. Milaeva, E.R.; Tyurin, V.Y.; Shpakovsky, D.B.; Moiseeva, A.A.; Gracheva, Y.A.; Antonenko, T.A.; Maduar, V.V.; Osolodkin, D.I.; Palyulin, V.A.; Shevtsova, E.F. Redox-active metal complexes with 2,2′-dipicolylamine containing ferrocenyl moiety: Synthesis, electrochemical behavior and biological activity. *J. Organomet. Chem.* **2017**, *839*, 60–70. [CrossRef]
9. Dwadnia, N.; Allouch, F.; Pirio, N.; Roger, J.; Cattey, H.; Fournier, S.; Penouilh, M.-J.; Devillers, C.H.; Lucas, D.; Naoufal, D.; et al. Aminomethyl-Substituted Ferrocenes and Derivatives: Straightforward Synthetic Routes, Structural Characterization, and Electrochemical Analysis. *Organometallics* **2013**, *32*, 5784–5797. [CrossRef]
10. Osakada, K.; Sakano, T.; Horie, M.; Suzaki, Y. Functionalized ferrocenes: Unique properties based on electronic communication between amino group of the ligand and Fe center. *Coord. Chem. Rev.* **2006**, *250*, 1012–1022. [CrossRef]
11. Fabbrizzi, L. The ferrocenium/ferrocene couple: A versatile redox switch. *ChemTexts* **2020**, *6*, 22. [CrossRef]
12. Bayly, S.R.; Beer, P.D.; Chen, G.Z. Ferrocene Sensors. In *Ferrocenes: Ligands, Materials and Biomolecules*; Stepnicka, P., Ed.; John Wiley & Sons: Chichester, UK, 2008; pp. 281–318.

13. Noviandri, I.; Brown, K.N.; Fleming, D.S.; Gulyas, P.T.; Lay, P.A.; Masters, A.F.; Phillips, L. The Decamethylferrocenium/Decamethylferrocene Redox Couple: A Superior Redox Standard to the Ferrocenium/Ferrocene Redox Couple for Studying Solvent Effects on the Thermodynamics of Electron Transfer. *J. Phys. Chem. B* **1999**, *103*, 6713–6722. [CrossRef]
14. Yang, Y.; Yu, L. Theoretical investigations of ferrocene/ferrocenium solvation in imidazolium-based room-temperature ionic liquids. *PCCP Phys. Chem. Chem. Phys.* **2013**, *15*, 2669–2683. [CrossRef]
15. Torriero, A.A.J. Characterization of decamethylferrocene and ferrocene in ionic liquids: Argon and vacuum effect on their electrochemical properties. *Electrochim. Acta* **2014**, *137*, 235–244. [CrossRef]
16. Torriero, A.A.J.; Sunarso, J.; Forsyth, M.; Pozo-Gonzalo, C. Assessment of permethylated transition-metal sandwich complexes as internal reference redox systems in ionic liquids. *PCCP Phys. Chem. Chem. Phys.* **2013**, *15*, 2547–2553. [CrossRef]
17. Torriero, A.A.J.; Howlett, P.C. Ionic liquid effects on the redox potential of ferrocene. *Electrochem. Commun.* **2012**, *16*, 84–87. [CrossRef]
18. Torriero, A.A.; Sunarso, J.; Howlett, P.C. Critical evaluation of reference systems for voltammetric measurements in ionic liquids. *Electrochim. Acta* **2012**, *82*, 60–68. [CrossRef]
19. Torriero, A.A.J. Reference systems for voltammetric measurements in ionic liquids. In *Electrochemistry in Ionic Liquids. Volume 1: Fundamentals*; Torriero, A.A.J., Ed.; Springer: Cham, Switzerland, 2015; Volume 1.
20. Torriero, A.A.J. On Choosing Ferrocene as an Internal Reference Redox Scale for Voltammetric Measurements: A Cautionary Tale. *Med. Anal. Chem. Int. J.* **2019**, *3*, 000151. [CrossRef]
21. Shvartsev, B.; Cohn, G.; Shasha, H.; Eichel, R.-A.; Ein-Eli, Y. Reference electrode assembly and its use in the study of fluorohydrogenate ionic liquid silicon electrochemistry. *PCCP Phys. Chem. Chem. Phys.* **2013**, *15*, 17837–17845. [CrossRef] [PubMed]
22. Inzelt, G.; Lewenstam, A.; Scholz, F. *Handbook of Reference Electrodes*; Springer: Berlin, Germany, 2013.
23. Bard, A.J.; Faulkner, L.R. *Electrochemical Methods: Fundamentals and Applications*, 2nd ed.; John Wiley & Sons, Inc.: New York, NY, USA, 2001.
24. Izutzu, K. *Electrochemistry in Nonaqueous Solutions*; Wiley-VCH: New York, NY, USA, 2002.
25. Smith, T.J.; Stevenson, K.J. Reference electrodes. In *Handbook of Electrochemistry*; Zoski, C.G., Ed.; Elsevier: Amsterdam, The Natherlands, 2007; pp. 73–110.
26. Ives, D.J.G.; Janz, G.J.; Ives, D.J.D. *Reference Electrodes, Theory and Practice*; Academic Press: London, UK, 1961.
27. Torriero, A.A.J. Understanding the Differences between a Quasi-Reference Electrode and a Reference Electrode. *Med. Anal. Chem. Int. J.* **2019**, *3*, 000144. [CrossRef]
28. Gritzner, G.; Kuta, J. Recommendations on reporting electrode potentials in nonaqueous solvents. *Pure Appl. Chem.* **1983**, *56*, 461–466. [CrossRef]
29. Torriero, A.A.J.; Feldberg, S.; Zhang, J.; Simonov, A.; Bond, A. On choosing a reference redox system for electrochemical measurements: A cautionary tale. *J. Solid State Electrochem.* **2013**, *17*, 3021–3026. [CrossRef]
30. Aranzaes, J.R.; Daniel, M.-C.; Astruc, D. Metallocenes as references for the determination of redox potentials by cyclic voltammetry—Permethylated iron and cobalt sandwich complexes, inhibition by polyamine dendrimers, and the role of hydroxy-containing ferrocenes. *Can. J. Chem.* **2006**, *84*, 288–299. [CrossRef]
31. Ruiz, J.; Astruc, D. Permethylated electron-reservoir sandwich complexes as references for the determination of redox potentials. Suggestion of a new redox scale. *Comptes Rendus De L'academie Des Sci. Ser. IIc Chim.* **1998**, *1*, 21–27. [CrossRef]
32. Matsumoto, M.; Swaddle, T.W. The Decamethylferrocene(+/0) Electrode Reaction in Organic Solvents at Variable Pressure and Temperature. *Inorg. Chem.* **2004**, *43*, 2724–2735. [CrossRef]
33. Freyberg, D.P.; Robbins, J.L.; Raymond, K.N.; Smart, J.C. Crystal and molecular structures of decamethylmanganocene and decamethylferrocene. Static Jahn-Teller distortion in a metallocene. *J. Am. Chem. Soc.* **1979**, *101*, 892–897. [CrossRef]
34. Barriere, F.; Geiger, W.E. Use of Weakly Coordinating Anions to Develop an Integrated Approach to the Tuning of $\Delta E_{1/2}$ Values by Medium Effects. *J. Am. Chem. Soc.* **2006**, *128*, 3980–3989. [CrossRef] [PubMed]
35. Bennett, M.A.; Bhargava, S.K.; Bond, A.M.; Burgar, I.M.; Guo, S.X.; Kar, G.; Priver, S.H.; Wagler, J.; Willis, A.C.; Torriero, A.A.J. Synthesis, X-ray structure and electrochemical oxidation of palladium(II) complexes of ferrocenyldiphenylphosphine. *Dalton Trans.* **2010**, *39*, 9079–9090. [CrossRef] [PubMed]
36. Zeng, Z.; Torriero, A.A.J.; Belousoff, M.J.; Bond, A.M.; Spiccia, L. Synthesis, X-ray Structure of Ferrocene Bearing bis(Zn-cyclen) Complexes and the Selective Electrochemical Sensing of TpT. *Chemistry* **2009**, *15*, 10988–10996. [CrossRef] [PubMed]
37. Blom, N.F.; Neuse, E.W.; Thomas, H.G. Electrochemical characterization of some ferrocenylcarboxylic acids. *Transit. Met. Chem.* **1987**, *12*, 301–306. [CrossRef]
38. Nonjola, P.T.N.; Siegert, U.; Swarts, J.C. Synthesis, Electrochemistry and Cytotoxicity of Ferrocene-Containing Amides, Amines and Amino-Hydrochlorides. *J. Inorg. Organomet. Polym. Mater.* **2015**, *25*, 376–385. [CrossRef]
39. Zhong, Z.H.; Matsumura-Inoue, T.; Ichimura, A. Solvent effect on the redox potential of ferrocene derivatives using an ultramicroelectrode. *Anal. Sci.* **1992**, *8*, 877–879. [CrossRef]
40. Paul, A.; Borrelli, R.; Bouyanfif, H.; Gottis, S.; Sauvage, F. Tunable Redox Potential, Optical Properties, and Enhanced Stability of Modified Ferrocene-Based Complexes. *ACS Omega* **2019**, *4*, 14780–14789. [CrossRef]
41. Scholl, H.; Sochaj, K. Cyclic voltammetry of some ferrocenophanes in acetonitrile. *Electrochim. Acta* **1991**, *36*, 689–694. [CrossRef]

42. Plenio, H.; Yang, J.; Diodone, R.; Heinze, J. Redox-Switched Bonding of Protons to Ferrocenophanes, Ferrocene Cryptands, and Simple Ferrocene Amines. Correlation of X-ray Structural Data and Cyclic Voltammetry Derived Redox Potentials. *Inorg. Chem.* **1994**, *33*, 4098–4104. [CrossRef]
43. Lee, T.-Y.; Chiang, P.-R.; Tsai, M.-C.; Lin, C.-Y.; Huang, J.-H. From diacetylferrocene to 1,1′-ferrocenyldiimines: Substituent effects on synthesis, molecular structure, electrochemical behavior and optical absorption property. *J. Mol. Struct.* **2009**, *935*, 102–109. [CrossRef]
44. Manfredi, N.; Decavoli, C.; Boldrini, C.L.; Coluccini, C.; Abbotto, A. Ferrocene Derivatives Functionalized with Donor/Acceptor (Hetero)Aromatic Substituents: Tuning of Redox Properties. *Energies* **2020**, *13*, 3937. [CrossRef]
45. Zapata, F.; Caballero, A.; Espinosa, A.; Tárraga, A.; Molina, P. Imidazole-Annelated Ferrocene Derivatives as Highly Selective and Sensitive Multichannel Chemical Probes for Pb(II) Cations. *J. Org. Chem.* **2009**, *74*, 4787–4796. [CrossRef] [PubMed]
46. Celedón, S.; Hamon, P.; Artigas, V.; Fuentealba, M.; Kahlal, S.; Carrillo, D.; Saillard, J.-Y.; Hamon, J.-R.; Manzur, C. Ferrocene functionalized enantiomerically pure Schiff bases and their Zn(II) and Pd(II) complexes: A spectroscopic, crystallographic, electrochemical and computational investigation. *New J. Chem.* **2022**, *46*, 3948–3960. [CrossRef]
47. Beer, P.D.; Gale, P.A.; Chen, G.Z. Electrochemical molecular recognition: Pathways between complexation and signalling. *J. Chem. Soc. Dalton Trans.* **1999**, 1897–1910. [CrossRef]
48. Beer, P.D.; Danks, J.P.; Hesek, D.; McAleer, J.F. A potassium-selective sulfide-linked redox-active ferrocene ionophore that exhibits extraordinary electrochemical recognition behaviour. *J. Chem. Soc. Chem. Commun.* **1993**, 1735–1737. [CrossRef]
49. Beer, P.D. Transition Metal and Organic Redox-Active Macrocycles Designed to Electrochemically Recognize Charged and Neutral Guest Species. In *Advances in Inorganic Chemistry*; Sykes, A.G., Ed.; Academic Press: Cambridge, MA, USA, 1992; Volume 39, pp. 79–157.
50. Pedersen, C.J. Cyclic polyethers and their complexes with metal salts. *J. Am. Chem. Soc.* **1967**, *89*, 7017–7036. [CrossRef]
51. Lindoy, L.F. *The Chemistry of Macrocyclic Ligand Complexes*; Cambridge University Press: Cambridge, UK, 1989.
52. Dobler, M. Macrocyclic chemistry: Aspects of organic and inorganic supramolecular chemistry by B. Dietrich, P. Viout and J.-M. Lehn. *Acta Crystallogr. Sect. B* **1993**, *49*, 1074. [CrossRef]
53. Beer, P.D.; Keefe, A.D.; Sikanyika, H.; Blackburn, C.; McAleer, J.F. Metallocene bis(aza-crown ether) ligands and related compounds. Their syntheses, coordination chemistry, and electrochemical properties. *J. Chem. Soc. Dalton Trans.* **1990**, 3289–3294. [CrossRef]
54. Saji, T.; Kinoshita, I. Electrochemical ion transport with ferrocene functionalized crown ether. *J. Chem. Soc. Chem. Commun.* **1986**, 716–717. [CrossRef]
55. Beer, P.D.; Sikanyika, H.; Slawin, A.M.Z.; Williams, D.J. The synthesis, coordination and electrochemical studies of metallocene bis(crown ether) receptor molecules. Single-crystal x-ray structure of a ferrocene bis(crown ether) potassium complex. *Polyhedron* **1989**, *8*, 879–886. [CrossRef]
56. Saji, T. Electrochemically switched cation binding in pentaoxa [13] ferrocenophane. *Chem. Lett.* **1986**, *15*, 275–276. [CrossRef]
57. Beer, P.D.; Sikanyika, H.; Blackburn, C.; McAleer, J.F.; Drew, M.G.B. Redox responsive crown ethers containing a direct link between the ferrocene redox-active centre and benzo crown ether. Crystal structure of a ferrocene benzo-15-crown-5 sodium complex. *J. Organomet. Chem.* **1988**, *356*, C19–C22. [CrossRef]
58. Beer, P.D.; Blackburn, C.; McAleer, J.F.; Sikanyika, H. Redox-responsive crown ethers containing a conjugated link between the ferrocene moiety and a benzo crown ether. *Inorg. Chem.* **1990**, *29*, 378–381. [CrossRef]
59. Jin, S.; Wang, D.; Jin, X.; Chen, G.Z. Intramolecular Electrostatics: Coulomb's Law at Sub-Nanometers. *ChemPhysChem* **2004**, *5*, 1623–1629. [CrossRef]
60. Hall, C.D. Macrocycles and Cryptands Containing the Ferrocene Unit. In *Ferrocenes: Homogeneous Catalysis, Organic Synthesis, Materials Science*; Togni, A., Hayashi, T., Eds.; VCH: New York, NY, USA, 1995; pp. 279–316.
61. Hall, C.D.; Sharpe, N.W.; Danks, I.P.; Sang, Y.P. Cyclic voltammetry studies on the complexation of metal cations by cryptands containing the ferrocene unit. *J. Chem. Soc. Chem. Commun.* **1989**, 419–421. [CrossRef]
62. Dennis Hall, C.; Chu, S.Y.F. Cyclic voltammetry of cryptands and cryptates containing the ferrocene unit. *J. Organomet. Chem.* **1995**, *498*, 221–228. [CrossRef]
63. Medina, J.C.; Goodnow, T.T.; Rojas, M.T.; Atwood, J.L.; Lynn, B.C.; Kaifer, A.E.; Gokel, G.W. Ferrocenyl iron as a donor group for complexed silver in ferrocenyldimethyl[2.2]cryptand: A redox-switched receptor effective in water. *J. Am. Chem. Soc.* **1992**, *114*, 10583–10595. [CrossRef]
64. Plenio, H.; Aberle, C. Oxaferrocene Cryptands as Efficient Molecular Switches for Alkali and Alkaline Earth Metal Ions. *Organometallics* **1997**, *16*, 5950–5957. [CrossRef]
65. Beer, P.D.; Crowe, D.B.; Ogden, M.I.; Drew, M.G.B.; Main, B. Ammonium redox-responsive receptors containing multiple ferrocene and quinone redox-active centres attached to di- and tri-aza crown ether macrocycles. *J. Chem. Soc. Dalton Trans.* **1993**, 2107–2116. [CrossRef]
66. Shi, L.; Song, W.; Li, Y.; Li, D.-W.; Swanick, K.N.; Ding, Z.; Long, Y.-T. A multi-channel sensor based on 8-hydroxyquinoline ferrocenoate for probing Hg(II) ion. *Talanta* **2011**, *84*, 900–904. [CrossRef]
67. Li, S.-H.; Chen, F.-R.; Zhou, Y.-F.; Wang, J.-N.; Zhang, H.; Xu, J.-G. Enhanced fluorescence sensing of hydroxylated organotins by a boronic acid-linked Schiff base. *Chem. Commun.* **2009**, 4179–4181. [CrossRef]

68. Zanello, P.; Cinquantini, A.; Fontani, M.; Giardiello, M.; Giorgi, G.; Landis, C.R.; Kimmich, B.F.M. Redox behavior of boronato-functionalized 1,1′-bis(diphenylphosphino)ferrocenes. *J. Organomet. Chem.* **2001**, *637–639*, 800–804. [CrossRef]
69. El Ghachtouli, S.; Cadiou, C.; Déchamps-Olivier, I.; Chuburu, F.; Aplincourt, M.; Turcry, V.; Le Baccon, M.; Handel, H. Spectroscopy and Redox Behaviour of Dicopper(II) and Dinickel(II) Complexes of Bis(cyclen) and Bis(cyclam) Ligands. *Eur. J. Inorg. Chem.* **2005**, *2005*, 2658–2668. [CrossRef]
70. Mruthunjaya, A.K.V.; Torriero, A.A.J. Mechanistic Aspects of the Electrochemical Oxidation of Aliphatic Amines and Aniline Derivatives. *Molecules* **2023**, *28*, 471. [CrossRef] [PubMed]
71. Zeng, Z.; Belousoff, M.J.; Spiccia, L.; Bond, A.M.; Torriero, A.A.J. Macrocycles Bearing Ferrocenyl Pendants and their Electrochemical Properties upon Binding to Divalent Transition Metal Cations. *ChemPlusChem* **2018**, *83*, 728–738. [CrossRef] [PubMed]
72. Zeng, Z.; Torriero, A.A.J.; Bond, A.M.; Spiccia, L. Fluorescent and Electrochemical Sensing of Polyphosphate Nucleotides by Ferrocene Functionalised with Two Zn(II)-(TACN)(pyrene) Complexes. *Chemistry* **2010**, *16*, 9154–9163. [CrossRef]
73. Plenio, H.; Aberle, C. Synthesis of a ferrocene bridged cyclam: A new redox-active macrocycle and the structure of a nickel(II) complex with strongly coupled metal centers. *Chem. Commun.* **1998**, 2697–2698. [CrossRef]
74. Plenio, H.; Aberle, C.; Al Shihadeh, Y.; Lloris, J.M.; Martínez-Máñez, R.; Pardo, T.; Soto, J. Ferrocene–Cyclam: A Redox-Active Macrocycle for the Complexation of Transition Metal Ions and a Study on the Influence of the Relative Permittivity on the Coulombic Interaction between Metal Cations. *Chemistry* **2001**, *7*, 2848–2861. [CrossRef]
75. Tendero, M.J.L.; Benito, A.; Cano, J.; Lloris, J.M.; Martínez-Máñez, R.; Soto, J.; Edwards, A.J.; Raithby, P.R.; Rennie, M.A. Host molecules containing electroactive cavities obtained by the molecular assembly of redox-active ligands and metal ions. *J. Chem. Soc. Chem. Commun.* **1995**, 1643–1644. [CrossRef]
76. Beer, P.D.; Smith, D.K. Tunable bis(ferrocenyl) receptors for the solution-phase electrochemical sensing of transition-metal cations. *J. Chem. Soc. Dalton Trans.* **1998**, 417–424. [CrossRef]
77. De Santis, G.; Fabbrizzi, L.; Licchelli, M.; Pallavicini, P.; Perotti, A. A redox-switchable ligand for which the binding ability is enhanced by oxidation of its ferrocene unit. *J. Chem. Soc. Dalton Trans.* **1992**, 3283–3284. [CrossRef]
78. Zapata, F.; Caballero, A.; Espinosa, A.; Tárraga, A.; Molina, P. A Simple but Effective Ferrocene Derivative as a Redox, Colorimetric, and Fluorescent Receptor for Highly Selective Recognition of Zn^{2+} Ions. *Org. Lett.* **2007**, *9*, 2385–2388. [CrossRef] [PubMed]
79. Nedunchezhian, K.; Nallathambi, S. Mono- and di-ferrocene conjugated 5-methyl benzimidazole based multi-channel receptors for cations/anions with their antimicrobial and anticancer studies. *New J. Chem.* **2023**, *47*, 4656–4666. [CrossRef]
80. Zhang, B.; Suo, Q.; Li, Q.; Hu, J.; Zhu, Y.; Gao, Y.; Wang, Y. Multiresponsive chemosensors based on ferrocenylimidazo[4,5-b]pyridines: Solvent-dependent selective dual sensing of Hg^{2+} and Pb^{2+}. *Tetrahedron* **2022**, *120*, 132878. [CrossRef]
81. Tian, H.-j.; Tang, R.-r.; Li, S.-f.; Luo, Y.-m. Synthesis, characterization and electrochemical recognition of metal ions of three new ferrocenyl derivatives containing pyridyl moiety. *J. Cent. South Univ.* **2013**, *20*, 3379–3384. [CrossRef]
82. Kaur, S.; Shalini, B.A.; Ahmad Shiekh, B.; Kumar, V.; Kaur, I. Triazole-tethered naphthalimide-ferrocenyl-chalcone based voltammetric and potentiometric sensors for selective electrochemical quantification of Copper(II) ions. *J. Electroanal. Chem.* **2022**, *905*, 115966. [CrossRef]
83. Arivazhagan, C.; Borthakur, R.; Ghosh, S. Ferrocene and Triazole-Appended Rhodamine Based Multisignaling Sensors for Hg^{2+} and Their Application in Live Cell Imaging. *Organometallics* **2015**, *34*, 1147–1155. [CrossRef]
84. Lopez, J.L.; Tárraga, A.; Espinosa, A.; Velasco, M.D.; Molina, P.; Lloveras, V.; Vidal-Gancedo, J.; Rovira, C.; Veciana, J.; Evans, D.J.; et al. A New Multifunctional Ferrocenyl-Substituted Ferrocenophane Derivative: Optical and Electronic Properties and Selective Recognition of Mg^{2+} Ions. *Chemistry* **2004**, *10*, 1815–1826. [CrossRef]
85. Otón, F.; Ratera, I.; Espinosa, A.; Wurtz, K.; Parella, T.; Tárraga, A.; Veciana, J.; Molina, P. Selective Metal-Cation Recognition by [2.2]Ferrocenophanes: The Cases of Zinc- and Lithium-Sensing. *Chemistry* **2010**, *16*, 1532–1542. [CrossRef]
86. Otón, F.; González, M.d.C.; Espinosa, A.; Tárraga, A.; Molina, P. Synthesis, Structural Characterization, and Sensing Properties of Clickable Unsymmetrical 1,1′-Disubstituted Ferrocene–Triazole Derivatives. *Organometallics* **2012**, *31*, 2085–2096. [CrossRef]
87. González, M.C.; Otón, F.; Orenes, R.A.; Espinosa, A.; Tárraga, A.; Molina, P. Ferrocene–Triazole–Pyrene Triads as Multichannel Heteroditopic Recognition Receptors for Anions, Cations and Ion Pairs. *Organometallics* **2014**, *33*, 2837–2852. [CrossRef]
88. Sola, A.; Otón, F.; Espinosa, A.; Tárraga, A.; Molina, P. Aldimines generated from aza-Wittig reaction between bis(iminophosphoranes) derived from 1,1′-diazidoferrocene and aromatic or heteroaromatic aldehydes: Electrochemical and optical behaviour towards metal cations. *Dalton Trans.* **2011**, *40*, 12548–12559. [CrossRef] [PubMed]
89. Guo, L.; Yan, L.; Xie, R.; Han, L.; Zhu, N. Multi-channel sensing of trivalent metal ions using a simple ferrocenyl Schiff base probe with AIE property. *J. Mol. Struct.* **2024**, *1295*, 136629. [CrossRef]
90. Bhatta, S.R.; Bheemireddy, V.; Vijaykumar, G.; Thakur, A. Triazole appended mono and 1,1′-di-substituted ferrocene-naphthalene conjugates: Highly selective and sensitive multi-responsive probes for Hg(II). *Sens. Actuators B Chem.* **2017**, *240*, 640–650. [CrossRef]
91. Bhatta, S.R.; Mondal, B.; Lima, S.; Thakur, A. Metal-coordination driven intramolecular twisting: A turn-on fluorescent-redox probe for Hg^{2+} ions through the interaction of ferrocene nonbonding orbitals and dibenzylidenehydrazine. *Dalton Trans.* **2019**, *48*, 8209–8220. [CrossRef] [PubMed]
92. Bhatta, S.R.; Pal, A.; Sarangi, U.K.; Thakur, A. Ferrocene appended fluorescein-based ratiomeric fluorescence and electrochemical chemosensor for Fe^{3+} and Hg^{2+} ions in aqueous media: Application in real samples analysis. *Inorganica Chim. Acta* **2019**, *498*, 119097. [CrossRef]

93. Romero, T.; Orenes, R.A.; Tárraga, A.; Molina, P. Preparation, Structural Characterization, Electrochemistry, and Sensing Properties toward Anions and Cations of Ferrocene-Triazole Derivatives. *Organometallics* **2013**, *32*, 5740–5753. [CrossRef]
94. Kamal, A.; Kumar, S.; Kumar, V.; Mahajan, R.K. Selective sensing ability of ferrocene appended quinoline-triazole derivative toward Fe (III) ions. *Sens. Actuators B Chem.* **2015**, *221*, 370–378. [CrossRef]
95. Pandey, R.; Gupta, R.K.; Shahid, M.; Maiti, B.; Misra, A.; Pandey, D.S. Synthesis and Characterization of Electroactive Ferrocene Derivatives: Ferrocenylimidazoquinazoline as a Multichannel Chemosensor Selectively for Hg^{2+} and Pb^{2+} Ions in an Aqueous Environment. *Inorg. Chem.* **2012**, *51*, 298–311. [CrossRef]
96. Kiran Kumar, C.; Trivedi, R.; Giribabu, L.; Niveditha, S.; Bhanuprakash, K.; Sridhar, B. Ferrocenyl pyrazoline based multichannel receptors for a simple and highly selective recognition of Hg^{2+} and Cu^{2+} ions. *J. Organomet. Chem.* **2015**, *780*, 20–29. [CrossRef]
97. Chen, L.; Cui, X.; Cheng, H.; Chen, X.; Song, M.; Tang, M.; Wei, D.; Wu, Y. Syntheses, structures of N-(substituted)-2-aza-[3]-ferrocenophanes and their application as redox sensor for Cu^{2+} ion. *Appl. Organomet. Chem.* **2012**, *26*, 449–454. [CrossRef]
98. Krishnapriya, K.R.; Sampath, N.; Ponnuswamy, M.N.; Kandaswamy, M. Synthesis and electrochemical sensing behaviour of a new ferrocene functionalized tet ′a′ macrocyclic receptor towards transition metal ions. *Appl. Organomet. Chem.* **2007**, *21*, 311–317. [CrossRef]